CHAPTER V

COMPARISON OF EXPERIMENTAL RESULTS WITH THEORETICAL PREDICTIONS

As mentioned in the Introduction (chapter I), one of the aims of the present investigation is to study the mechanism of emission of nucleons and complex particles from excited nuclei. There are two ways of achieving this aim: (i) by on-line studies of energy spectra and angular distributions of different particles emitted in nuclear reactions using coincidence techniques wherever necessary and (ii) by off-line studies of excitation functions of several reactions involving nucleons and complex particle emission. Obviously the first method requires a very sophisticated apparatus and a lot of accelerator beam time to study several reactions. On the other hand, the second method is simpler, requires the least possible accelerator time if stacked foil activation technique is employed and at the same time enables a global study of a variety of reactions spanning a wide range of target nuclei and excitation energy. In both cases, the experimental observations have to be compared with theoretical predictions (based on different models) to elucidate the reaction mechanism.

The observed excitation functions show a high energy tail following the usual compound nucleus bump at low energy. The chief aim of the present investigation is to test models globally with regard to their applicability, to several types of alpha particle induced reactions, in light, medium and heavy target isotopes. For the success of such a comparison, accurate experimental data is needed. The excitation functions have been calculated theoretically using the statistical model with and without the inclusion of preequilibrium emission of particles according to hybrid model of Blann(ALICE/90). This model provides closed form expression, which inherently includes integration over the emitted particle energy and angular distribution, so that integral cross section at each energy and its variation with energy can be readily calculated in the form of theoretical excitation function.

The basic idea of the model is that only a few degrees of freedom are initially excited in a nuclear reaction and that the relaxation of the excited compound system occurs through a series of binary collisions. The energy brought in by the projectile is first shared between a few nucleons (or holes in the Fermi-sea) called excitons, and later redistributed over the whole nucleus through successive two-body collisions, creating a hierarchy of new intermediate states called 'door way' states and culminating in the formation of the equilibrium compound nucleus. The notable feature introduced into the model is that there exists a finite probability for particle emission at each intermediate stage, whereas in the compound nucleus model, such emission is not envisaged until the equilibrated compound nucleus is formed. Thus, while the equilibration is continuing on the one hand, particles are emitted into the continuum and such preequilibrium particles would naturally have higher energies than those subsequently emitted by the evaporation of the compound nucleus. As far as alpha-particle interaction with a nucleus is concerned, the mechanism of mode of reaction has been a point of interest for several years. It was experimentally found that the equilibrium statistical model underestimates the probability of particle emission whenever the incident particle energy is greater than a few tens of MeV. The so called " hard component" of the particle spectra and the "high energy tail" of the experimental excitation functions can not be reproduced by the equilibrium statistical model.

In the present work, the excitation functions of twenty three α-particle induced reactions have been studied. Of these there are six reactions [^{121}Sb(α,αn) + ^{123}Sb(α,α3n), ^{115}In(α,n), ^{113}In(α,n) + ^{115}In(α,3n), ^{115}In(α, 2p)] in which, the cross sections of only either the ground state or the meta stable state were measured. Hence these reactions were not compared with theory because their total cross sections have not been measured in this work. Thus in remaining seventeen reactions of the type (α,xnypzα) involving neutrons, protons and α-particles in

the exit channel, the comparison between theoretical and experimental results have been made.

The theoretical excitation functions including an equilibrium and preequilibrium contributions were calculated using the code ALICE/90. Blann, who was continuously improving his computer code on Hybrid model /1/, in 1984 introduce new algorithms into the code ALICE/85/300 /2/ to calculate multiple chance preequilibrium emission /3/. Later on, Kataria et al /4/ have incorporated a shell dependent level density formula due to Kataria, Ramamurthy and Kapoor /5/ into the above code which is known as ALICE/90. Owing to the semiclassical nature, the Hybrid model, involve a large number of physical parameters as well as a few adjustable parameters. The model predictions of course depend on the input values given to these parameters. A short description of the options chosen is given below.

The nuclear masses were calculated from the Myers and Swiatecki /6/ mass formula considering a liquid drop with the shell correction term without pairing (i.e. level density pairing is absorbed in the binding energies). The inverse cross sections were calculated using the optical model subroutine included in the code which uses the Becchetti and Greenless /7/ optical model parameters. The Fermi level density used is of the form

$$\rho(u) = \sqrt{\pi}/12\ (u-\delta)^{-5/4}\ a^{-1/4} \exp\ [\ 2\sqrt{a(u-\delta)}]$$

where u is the residual nuclear excitation energy, a is the level density parameter taken as A/9 MeV^{-1}, which is the default option of the code and $\delta = 11/A^{1/2}$ MeV the pairing energy shift, with either a back-shifted or standard shift option. We have used the standard option. The equilibrium part was calculated using standard Weisskopf and Ewing /8/ formalism. The statistical part of the code can account for

a large variety of reaction types. Besides evaporation of neutrons and protons also clusters such as deuteron and alpha particles can be considered. However, it has long been known that yields of nuclides with closed or nearly closed nucleon shells are not predicted well when standard Fermi gas level densities are used in the "evaporation" phase of deexcitation calculation /9,10/. In such cases (eg. target element Fe in present case) shell-dependent level density formula due to Kataria, Ramamurthy and Kapoor /5/ was used, which is incorporated into the code. This model relates the shell effects in the nuclear level densities to the shell correction term of the nuclear mass surface. Because the code contains a library of experimental masses as well as a liquid drop mass formula, the necessary shell correction terms can be generated internally requiring no effort on the part of the user.

There are three main points for discussion when using the Hybrid model option of ALICE:

(i) the initial exciton configuration

(ii) the intranuclear transition rate and

(iii) the mean free path multiplier

In the apriori formulation of the Hybrid model, the intranuclear transition rates are calculated either from the imaginary part of the optical model or from the free nucleon-nucleon scattering cross section /11/. The use of optical potential in calculating intranuclear transition rates for preequilibrium decay offers distinct advantages at least in principle over the nucleon-nucleon scattering approach. Specifically, the parameters of the optical potential have been determined from the results and trends of a large body of experimental data. The mean free path values are therefore based on experimental measurements in nuclear matter as opposed to the extrapolation of free scattering cross sections to the nuclear environment.

Secondly the question of possible errors in nucleon-nucleon scattering approach due to inability to consider recoil momentum effects are avoided by using the optical potential. Becchetti and Greenless /7/ analysed a vast amount of data to find a best set of optical-model parameters for nucleon-induced reactions. However, for particle energies exceeding 55 MeV, the optical model parameter of Becchetti and Greenless are no longer applicable and thus at higher energies the mean free path for intranuclear transitions must be calculated from nucleon-nucleon scattering cross sections. The mean free path multiplier 'K' which is a free parameter originally introduced by Blann /12/ to account for the transparency of nuclear matter in the lower density periphery was kept equal to unity.

It is customary to use the initial exciton number n_0 separated into proton and neutron excitons (n_p and n_n respectively) above and a hole n_h below the Fermi level as a fit parameter to match the theoretical predictions with the experimentally observed shape of the spectra and excitation functions. A good guess would be the number of nucleons in the projectile or an additional particle/hole or both /13-17/. For the incident α-particle used in the present work a reasonable choice for the initial exciton configuration is n_0= 4(4p0h), n_0=5(5p0h) and n_0=6(5p1h). All three were tested against the experimentally measured excitation functions to pick out the best out of them, and to draw inferences based on these comparisons individually for each reaction at first. For ease in comparison the twenty three reactions are studied in the present work are divided into three categories:

(i) those involving only neutrons emission (α, xn)

(ii) those involving neutrons and protons emission (α,pxn)

(iii) those involving α-particles and neutrons emission (α,αxn)

The comparison of each class is presented element wise, with all initial exciton configurations, where n_0 = 4(4p0h), n_0 = 5(5p0h) and n_0 = 6(5p1h)

configurations have been shown by a broken line (—— ——), a dot dashed line (— · — · — ·), a double dot dashed line (— ·· — ·· —) respectively and Weisskopf-Ewing estimates by a dashed line (– – – – –) together with present experimental results shown by solid circle with error bars.

V.1. (α,xn) Type of Reactions:

Since the neutron is uncharged and has no difficulty in passing through the Coulomb barrier, reactions involving emission of only neutrons have by far the best chance of being observed. They have generally the largest cross sections among the three types of reactions mentioned above. The excitation functions of these reactions are characterized by an initial exponential rise in the cross section, with energy begining from the threshold energy of the reaction. In this part of the excitation function the increasing energy of the projectile facilitates its penetration through the Coulomb barrier of the target nucleus, and the cross section reaches the maximum (peak) at an energy roughly correspondingly to the sum of the threshold energy and the Coulomb potential . At this energy the probability for the formation of a compound nucleus is maximum, and therefore it is loosely called the compound nucleus peak or maximum. Further increase in energy however, in the compound nucleus picture, the cross section again falls, rather exponentially, because of the competition due to multi-neutron emitting reactions. The so called bell shape of the excitation function, which is the hall mark of the compound nucleus mechanism, is seen in the theoretical Weisskopf-Ewing estimates.

Any departure from this traditional shape is an indication of the onset of a new reaction mechanism, that is how the high energy tails observed in the experimental excitation functions, are taken to the signatures of a non-equilibrium

reaction mechanism as against the conventional compound nucleus model. In an attempt to understand the reaction mechanism, a comparison is made between the theoretical predictions of preequilibrium model and the experimentally observed excitation functions. The details of this comparison is presented below for each reaction.

V.1.1 Target Element Gold:

(i) $^{197}Au(\alpha, n)^{200}Tl$ reaction :

The excitation function for this reaction measured in the present work is compared with the theoretical excitation functions based on Hybrid model for the initial exciton number n_0= 4,5,6 and Weisskopf-Ewing estimates as shown in figure V.1. It can be seen from figure, that the Weisskopf-Ewing estimates underestimate the low energy cross sections by an order of magnitude or more (which is multiplied by a factor ten in the present case), and emphasize the importance of non-equilibrium effects above 30MeV of bombarding energy. Thus, the Hybrid model with n_o=4(4p0h) is able to explain very satisfactorily the high energy tail observed in the measured excitation function.

An initial exciton configuration, n_0= 4(4p0h) signifies that only four excitons share the initial excitation energy at the instant of first projectile-target interaction. The four nucleons of the projectile are the most likely candidates to be endowed with the excitation energy and this picture is consistent with the alpha particle as the projectile.

It is also, however, possible in the Fermi-gas picture of the nucleus that an initial configuration n_0=5(5p0h) or n_0= 6(5p1h) may occur for the same projectile.

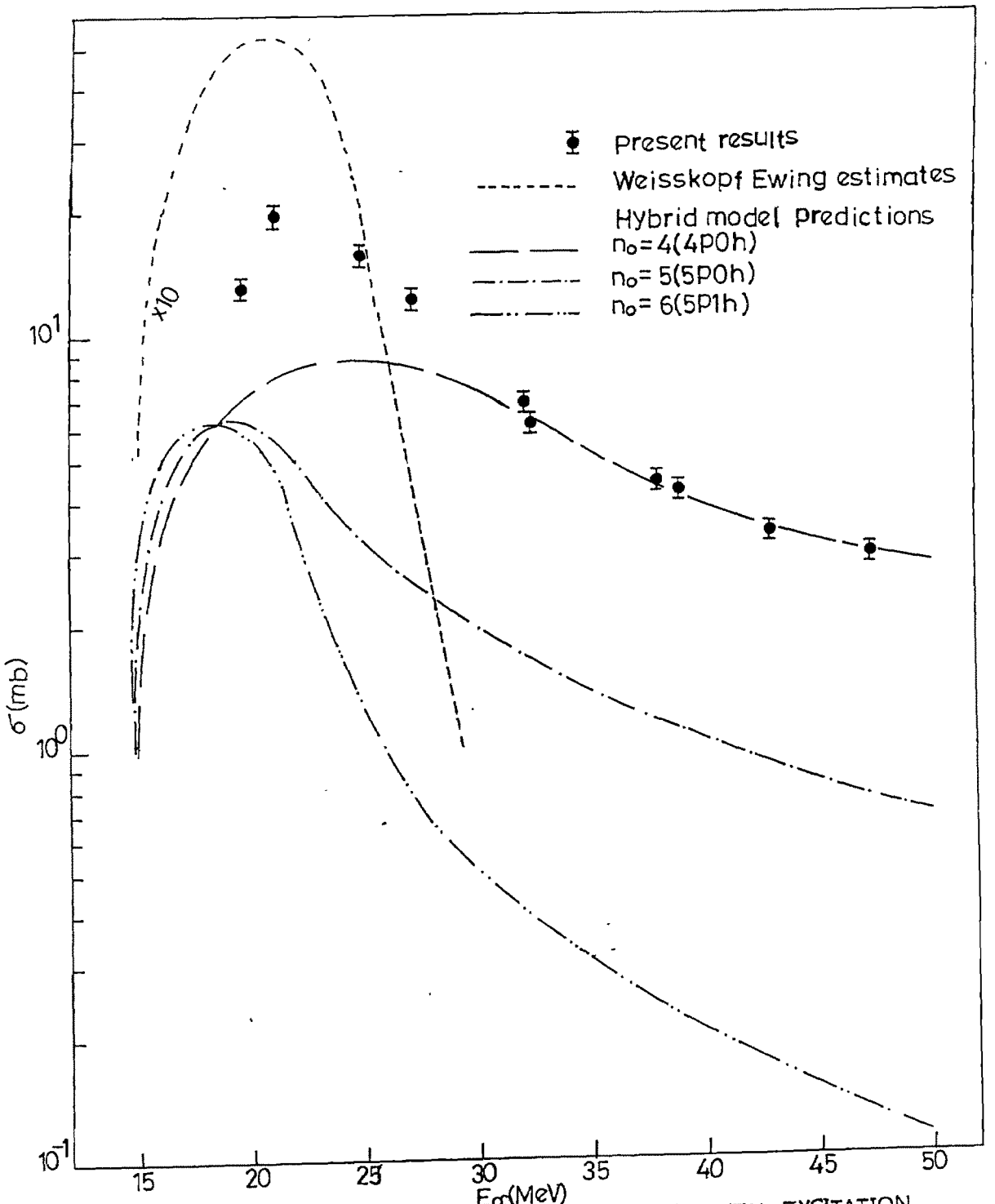

Fig.V.1 COMPARISON OF THEORETICAL AND EXPERIMENTAL EXCITATION FUNCTION OF $^{197}Au(\alpha,n)^{200}Tl$ REACTION

The physical interpretation is that, of the very first target-projectile interaction, in addition to the four excitons, an additional particle from the Fermi surface or an additional particle-hole pair from the Fermi-sea is created, respectively, in the initial exciton configurations n_0=5(5p0h) and n_0=6(5p1h), which is also shown in figure V.1.

It is well known that value of level density parameter 'a' shows local variations, particularly in the vicinity of magic numbers, thereby affecting the compound nucleus part of the cross section dominating at lower energies. Consequently, the maximum in the experimental excitation function occurring due to the compound nucleus is matched with theoretical Weisskopf-Ewing estimates by adjusting the value of the level density parameter 'a' approximately. We varied level density 'a' as A/7, A/8, A/9, A/10, A/12 MeV^{-1} to reproduce the compound nucleus peak respectively after fixing the initial exciton configuration. However all the values of level density parameter are not able to match the experimental compound nucleus peak of excitation function. The variation is only about 10%. Based on these consideration, the value of level density parameter 'a' for the theoretical calculations was chosen as global parameter A/9 MeV^{-1}.

(ii) ^{197}Au (α, 2n)^{199}Tl reaction :

The experimental and theoretical excitation functions for this reaction are shown in figure V.2. In this case, as seen from figure, while the theoretical shape for n_0=4(4p0h) agrees well with experimental shape of the excitation function, there is a systematic underestimation by about 30-40% of the experimental cross sections at high energy region. It may appear that the use of a fractional exciton number may yield a better result, but this should require the admixtures of an initial exciton states n_0=3, which is unphysical for a projectile like alpha particle.

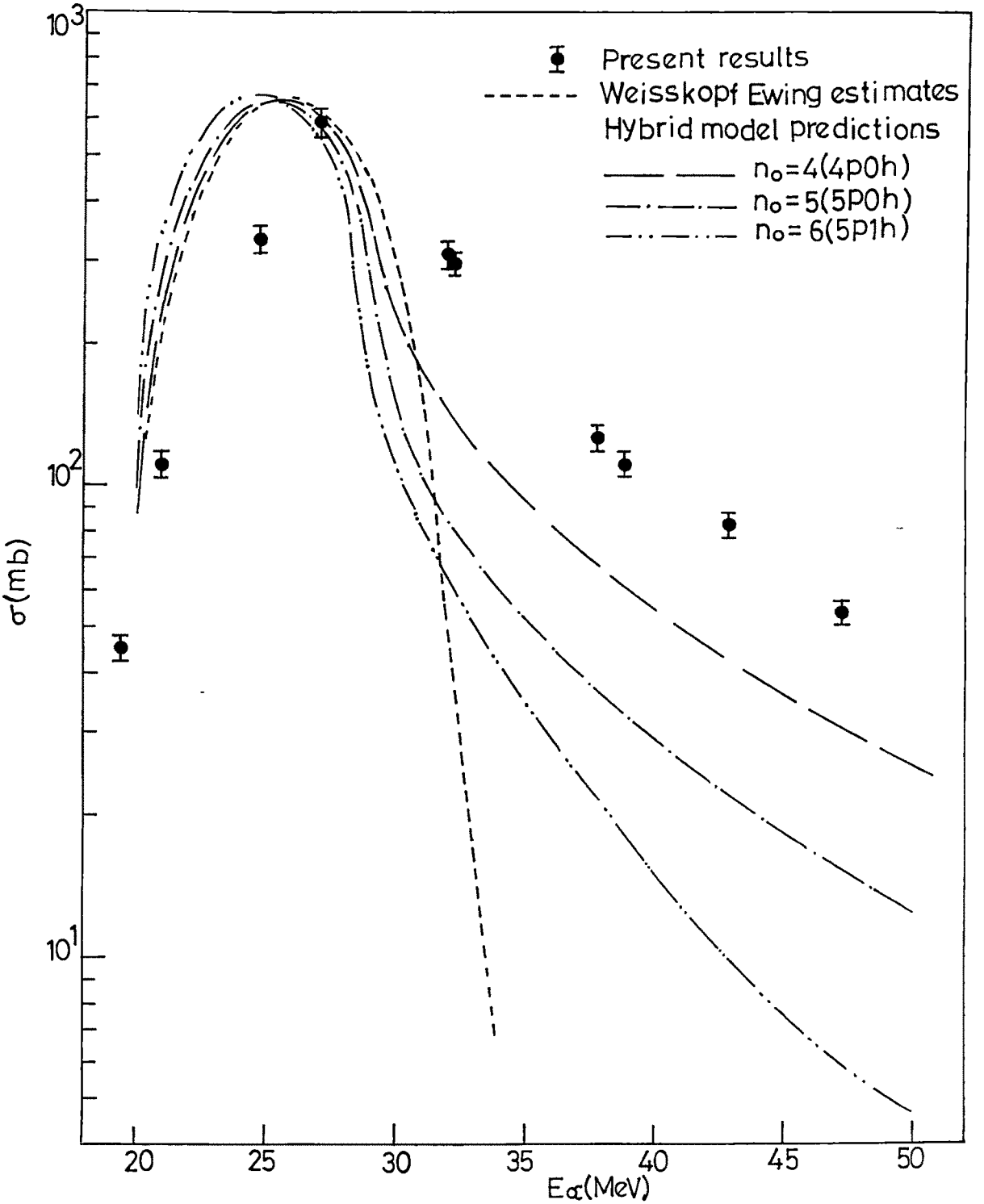

Fig.V.2 COMPARISON OF THEORETICAL AND EXPERIMENTAL EXCITATION FUNCTION OF $^{197}Au(\alpha,2n)^{199}Tl$ REACTION

The cross sections obtained by n_0 = 5(5p0h) and n_0 = 6(5p1h) configurations were lower than those obtained with n_0 = 4(4p0h) as shown in figure V.2. The Weisskopf-Ewing estimates fall of rapidly around 30MeV and show that preequilibrium emission dominates in the energy region 30-50MeV.

(iii) $^{197}Au(\alpha,3n)^{198}Tl$ reaction :

The comparison of present experimental excitation function with the theoretical predictions are shown in figure V.3. It can be seen from figure that the model predicts the shape of the excitation functions rather well in the preequilibrium dominated region but, however, it underestimates the cross sections. There is a shift in energy between the theoretical and experimental compound nucleus peak. It may appear that by shifting the theoretical curve to the right, by about 4 MeV may yield a better agreement, but there is no mechanism in the code by which this can be done simultaneously for equilibrium and preequilibrium contributions, as these two are separately calculated. Furthermore, such an attempt singles out a particular reaction, with special assumptions, made in its theoretical computations and in a global comparison like the present one, such special assumptions are sought to be avoided.

There is a shift in the energy between theoretical and experimental compound nucleus peaks of above two reactions. Generally such shifts are ascribed due to complete neglect of angular momentum effects in the Weisskopf-Ewing theoretical calculations provided in the code. Compound systems attained with incident particles of different masses have appreciably different angular momenta when excited to the same excitation energy. Thus, in principle, can lead to differences in the excitation function. If, in the last stages of nucleon deexcitation, high angular momentum inhibits particle emission more than it does γ-ray emission, then the peak of the excitation function corresponding to the particle emitting mode,

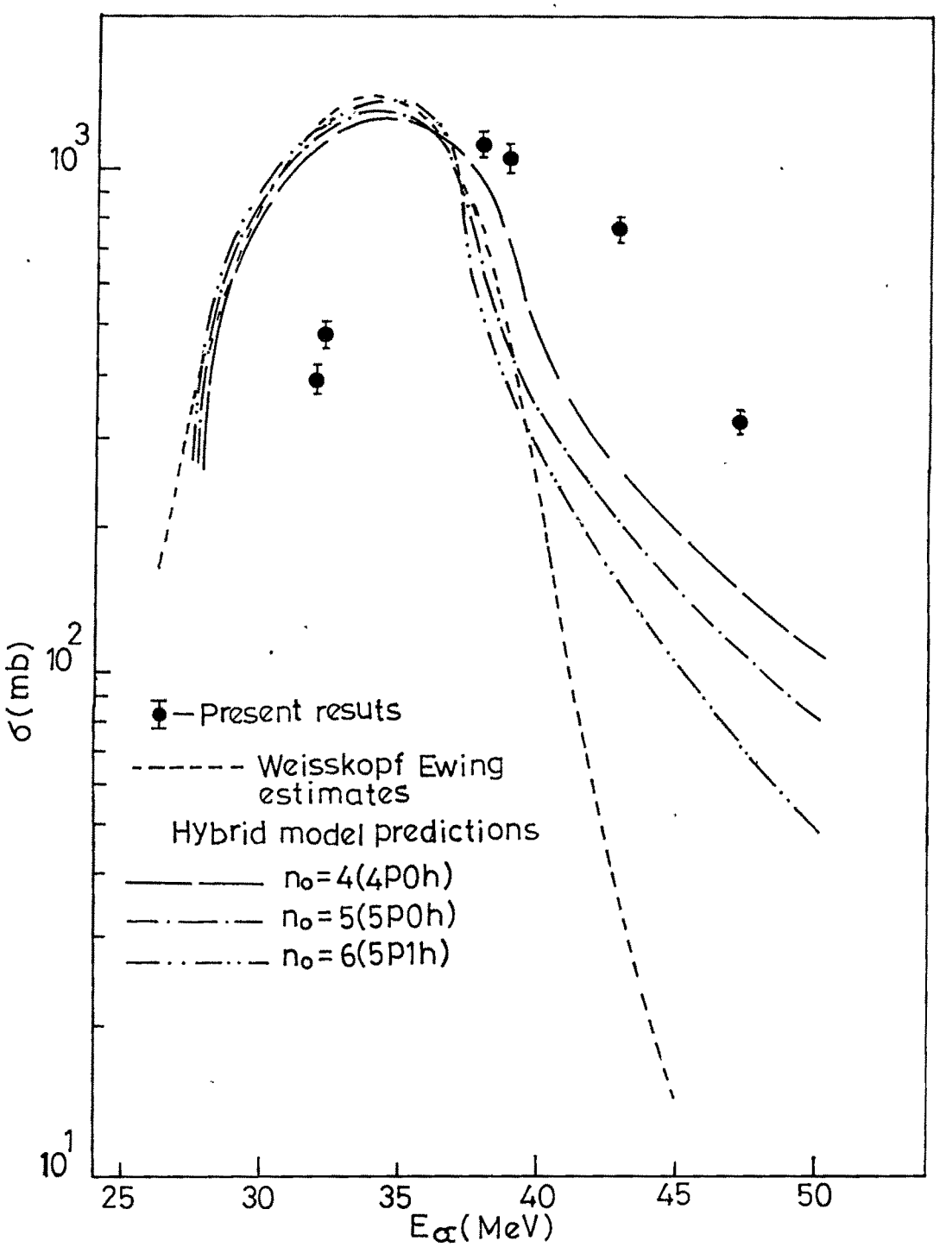

Fig.V.3 COMPARISON OF THEORETICAL AND EXPERIMENTAL EXCITATION FUNCTION OF $^{197}Au(\alpha,3n)^{198}Tl$ REACTION

will be shifted to higher energy side. Such shifts could also be produced if the mean energy of the evaporated particles increases with increasing nucleon spin. Blann and Merkel /18/ have indicated that inclusion of angular momentum effects broadens the excitation function. The order of magnitude of this shift can be obtained from nuclear rotational energy.

V.1.2 Target Element Antimony :

(i) $[^{121}Sb(\alpha,n) + ^{123}Sb(\alpha,3n)]^{124}I$ reactions :

As mentioned in the previous chapter IV.2.1, consequent on the use of natural antimony target, the excitation function for the production of ^{124}I is the weighted average of the above pair of reactions i.e. $^{121}Sb(\alpha,n)$ and $^{123}Sb(\alpha,3n)$.

Figures V.4 and V.5 show the experimental and theoretical excitation functions for the pair of reactions ^{121}Sb (α,n) and $^{123}Sb(\alpha,3n)$ respectively. As discussed in the chapter III.3.5, the individual cross sections are separated at high energies using eqn.(11) and eqn.(12). It is observed that Weisskopf-Ewing estimates accounted fairly well for the low energy compound nucleus dominated part of the excitation function, but failed to account for the observed cross sections at high energies where non-equilibrium effects predominate, beyond a few tens of MeV of bombarding energy. It can be seen that experimental results are consistent with the theoretical prediction of the Hybrid model with an initial exciton number n_0=4(4p0h).

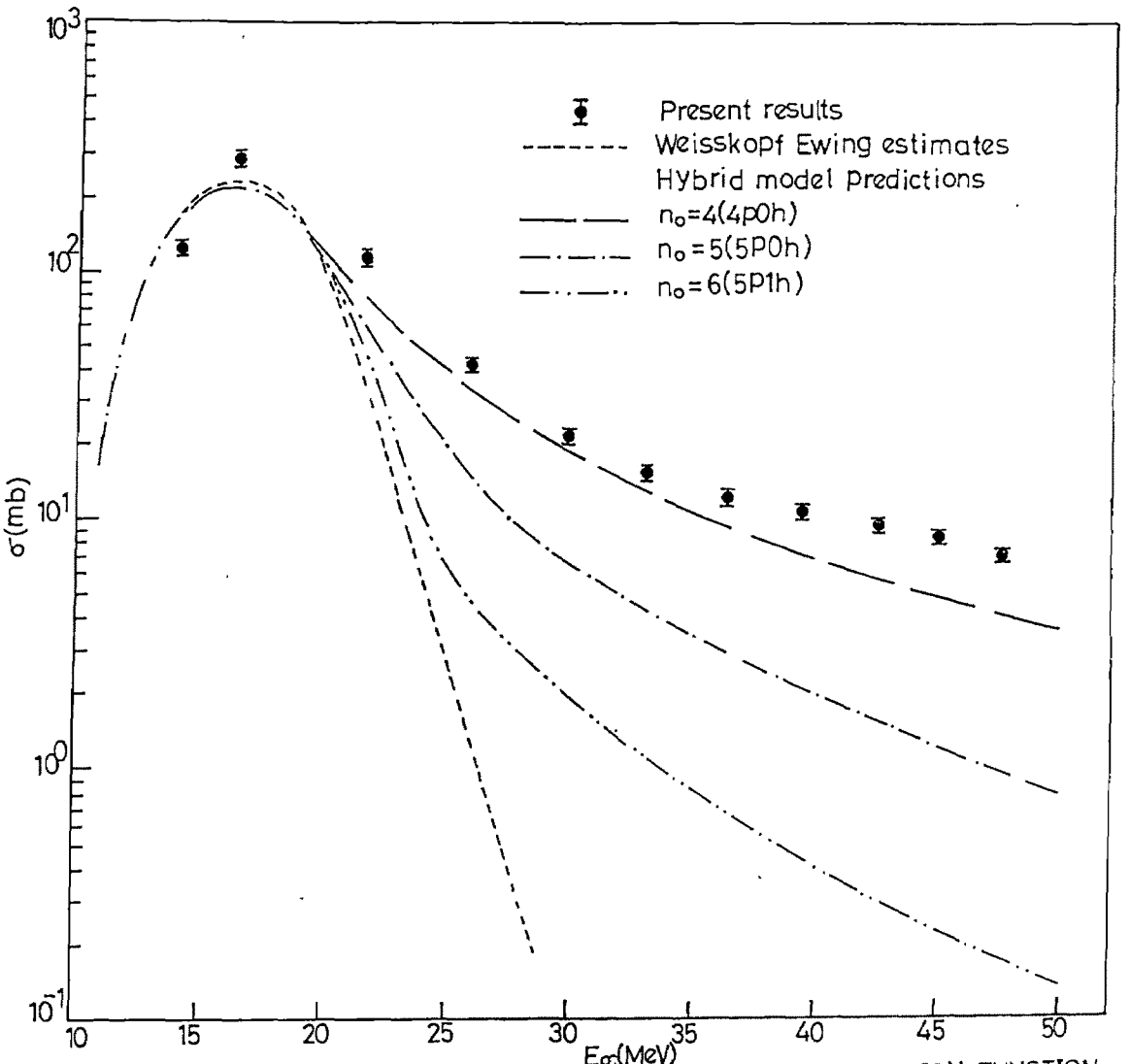

Fig.V.4 COMPARISON OF THEORETICAL AND EXPERIMENTAL EXCITATION FUNCTION OF $^{121}Sb(\alpha,n)^{124}I$ REACTION.

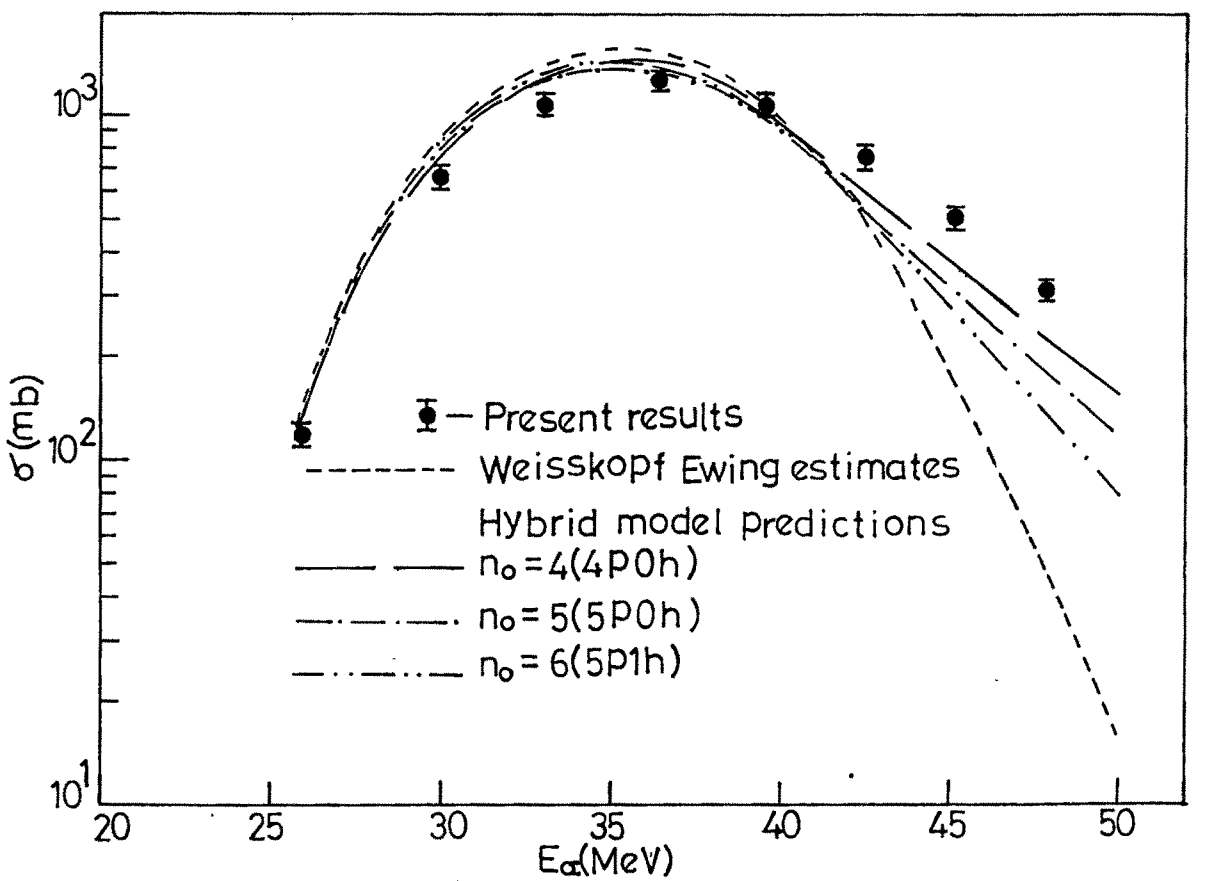

Fig.V.5 COMPARISON OF THEORETICAL AND EXPERIMENTAL EXCITATION FUNCTION OF $^{123}Sb(\alpha, 3n)^{124}I$ REACTION.

(ii) $[^{121}Sb(\alpha,2n)+^{123}Sb(\alpha,4n)]^{123}I$ reactions :

As, discussed previously, the excitation functions of the reactions $^{121}Sb(\alpha,2n)$ and $^{123}Sb(\alpha,4n)$, leading to residual nucleus ^{123}I, are separated using theoretical cross section values in the eqn.(11) and eqn.(12) of chapter III.3.5. The separated excitation functions are shown in figures V.6 and V.7 together with Weisskopf-Ewing and Hybrid model predictions respectively.

As shown in figure V.6 the predictions of the n_0=5(5p0h) and n_0=6(5p1h) configurations are lower than those obtained with n_0=4(4p$_0$h). It can be seen that, there is a good agreement between experimental and theoretical excitation functions corresponding to n_0 = 4(4p0h) over the whole energy region, reproducing the equilibrium and preequilibrium contributions. This is also in agreement with the findings of Djalaesis et al /16/, Michel and Brinkmann /14/, Gadioli et al /17/ and Singh et al /15/ who recommended the general application of n_0=4(4p0h). The physical interpretation of an initial exciton configuration n_0=4(4p0h) is that only four excitons initially share the excitation energy, which is equivalent to break-up of the incoming alpha particle in the field of the nucleus and the nucleons occupying excited states above the Fermi energy.

(iii) $^{121}Sb(\alpha,4n)^{121}I$ reaction :

Figure V.8 shows the excitation function for $^{121}Sb(\alpha,4n)$ reaction together with the theoretical excitation functions based on Hybrid model and Weisskopf-Ewing estimates. The threshold energy for this reaction is rather large (i.e 34.42 MeV) and as such there are only a few energy points in the initial rising part of the

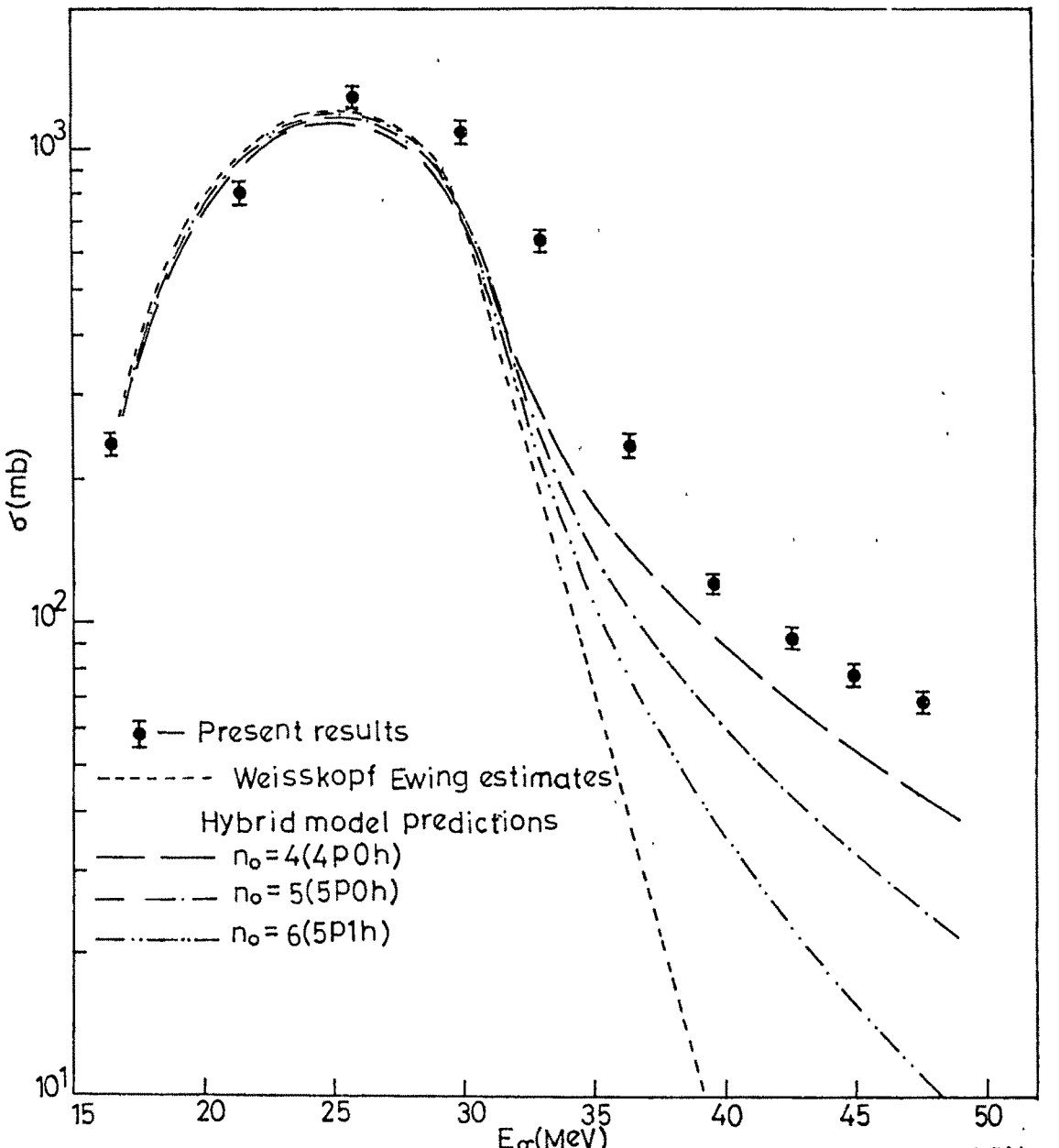

Fig·V·6 COMPARISON OF THEORETICAL AND EXPERIMENTAL EXCITATION FUNCTION OF $^{121}Sb(\alpha,2n)^{123}I$ REACTION.

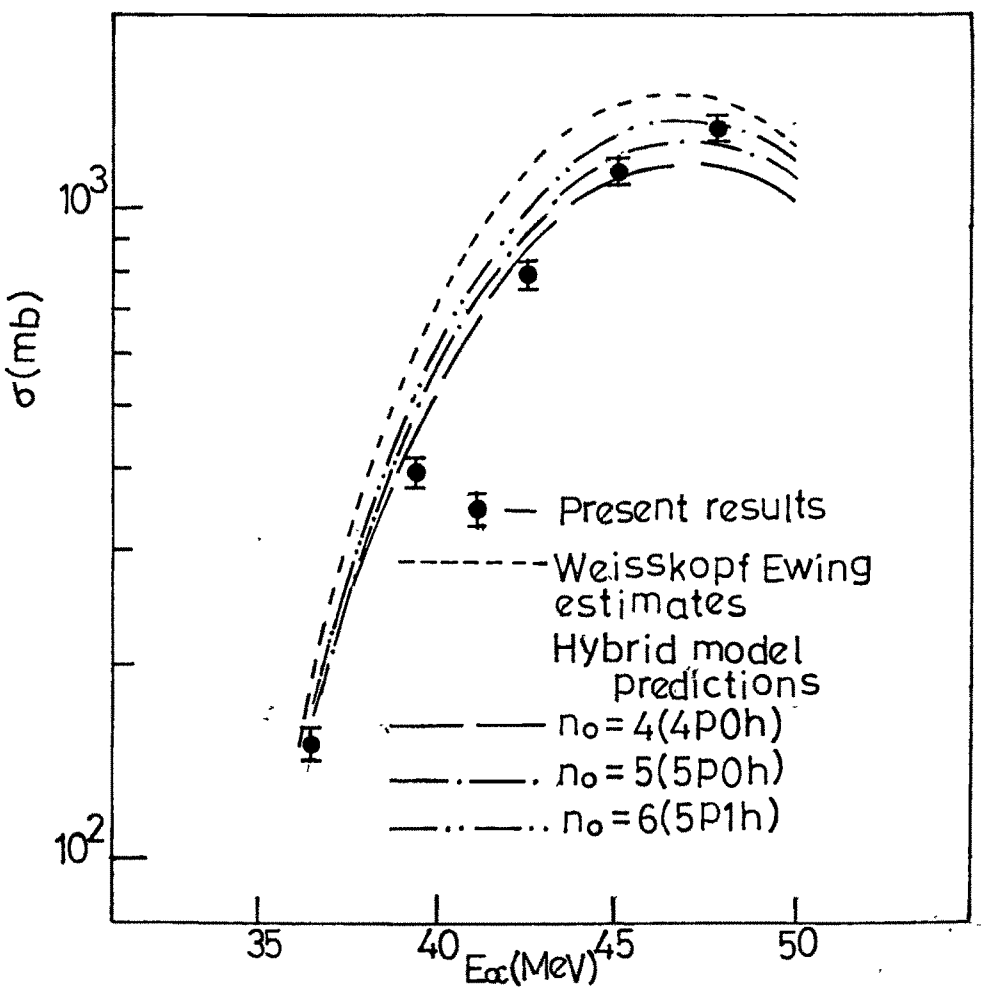

Fig.V.7 COMPARISON OF THEORETICAL AND EXPERIMENTAL EXCITATION FUNCTION OF $^{123}Sb(\alpha,4n)^{123}I$ REACTION

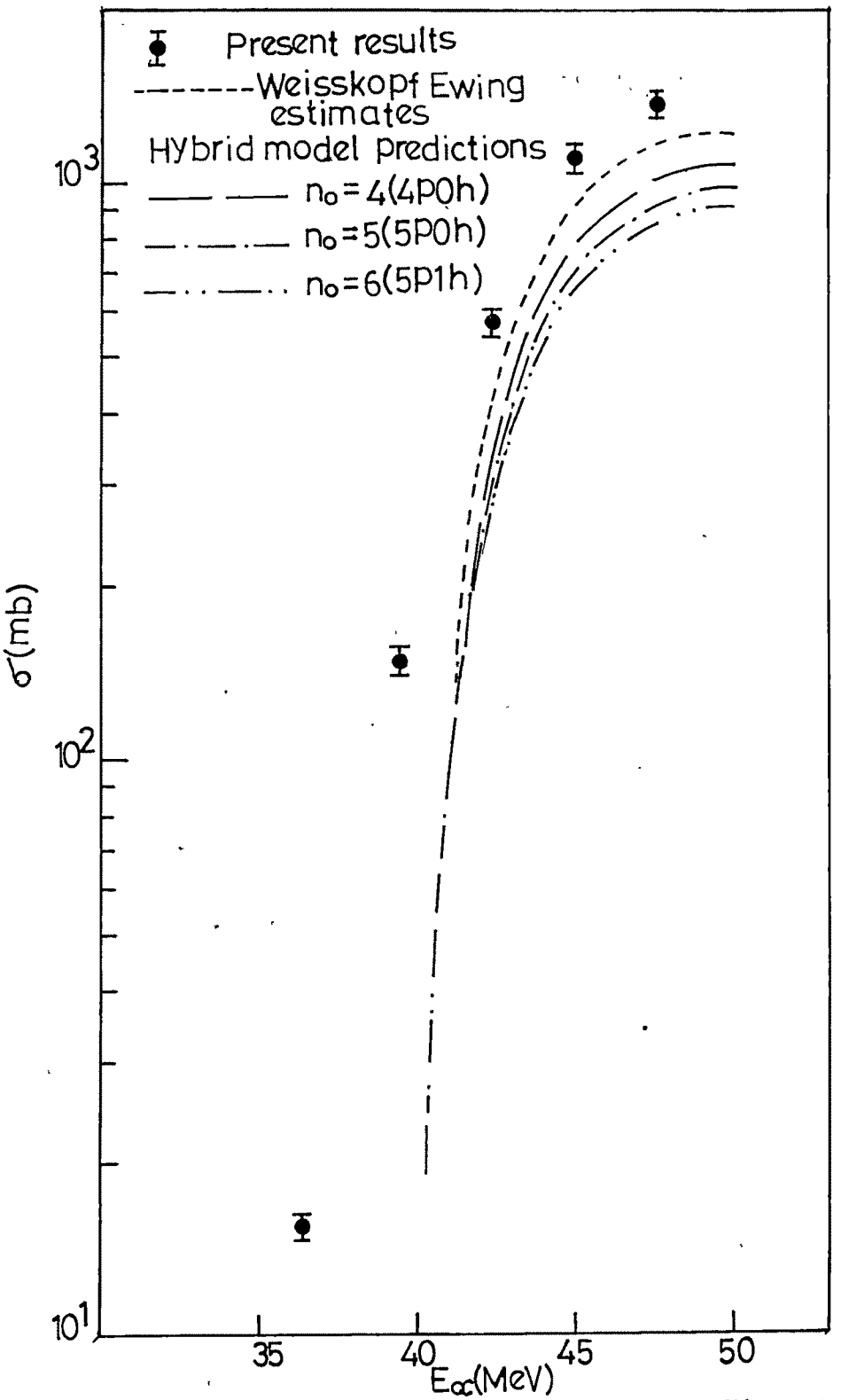

Fig.V.8 COMPARISON OF THEORETICAL AND EXPERIMENTAL EXCITATION FUNCTION OF $^{121}Sb(\alpha,4n)^{121}I$ REACTION.

experimental excitation function. In this region the preequilibrium model predictions are not very sensitive as the compound nucleus mechanism dominates.

V.1.3 Target Element Indium:

(i) $^{115}In(\alpha,2n)^{117}Sb$ reaction :

The presently measured excitation function of $^{115}In(\alpha,2n)^{117}Sb$ reaction is shown in figure V.9 together with Weisskopf-Ewing estimates and the Hybrid model predictions for initial exciton configurations n_0=4(4p0h), 5(5p0h) and 6(5p1h) respectively. It was observed that beyond 30 MeV non-equilibrium effects predominate, whereas the equilibrium compound nucleus predictions failed to predict the higher energy part of the excitation function. The cross sections obtained by the n_0=4(4p0h) configuration gives, in general, better agreement than other two configurations. The cross sections obtained by the n_0=5(5p0h) and n_0=6(5p1h) configurations are lower than those obtained with n_0 = 4(4p0h) as shown in figure.

It can be seen from the figure that the shape of excitation function is fairly well reproduced by n_0=4(4p0h) configuration, but its magnitude is under estimated by a factor of three in high energy region. It may appear that the use of a fractional exciton number may yield a better agreement, but this should require the admixture of an initial exciton states n_0=3, which is unphysical for a projectile like an alpha particle. It may appear that by shifting the theoretical curve to the right, by about 3 MeV yiels a better agreement, but there is no mechanism in the code by which this can be done, simultaneously for equilibrium and preequilibrium contributions, as these two are separately calculated. Further more, such an attempt signles out a particular reaction with special assumptions made in its theoretical computations and

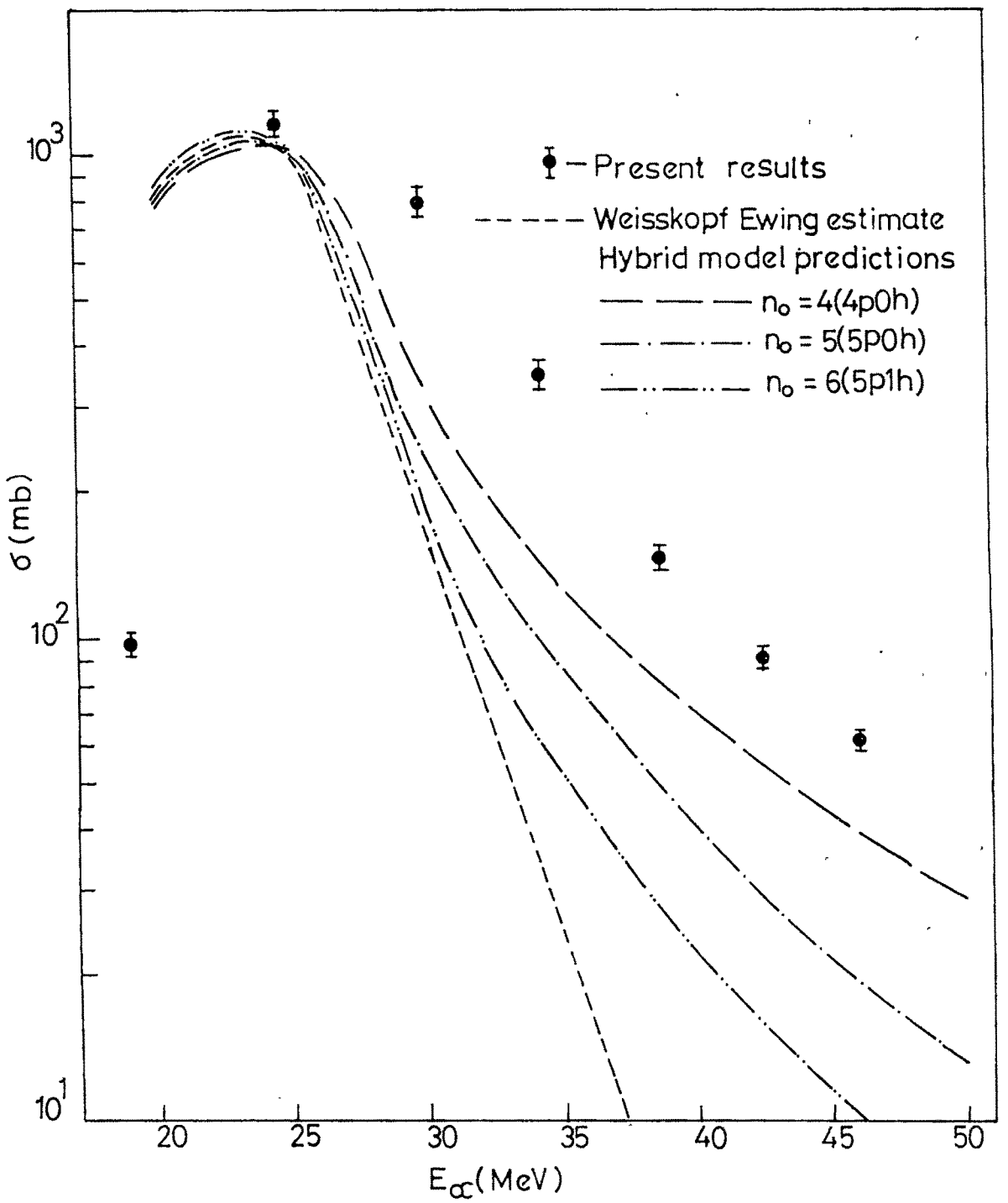

Fig.V.9 COMPARISON OF THEORETICAL AND EXPERIMENTAL EXCITATION FUNCTION OF $^{115}In(\alpha, 2n)^{117}Sb$ REACTION

in a global comparison like the present one, such special assumptions are sought to be avoided.

V.1.4 Target Element Iron:

(i) $^{56}Fe(\alpha,3n)^{57}Ni$ reaction :

Figure V.10 shows the excitation function for $^{56}Fe(\alpha,3n)^{57}Ni$ reaction together with the theoretical calculations based on Weisskopf-Ewing estimates and Hybrid model predictions using initial exciton configurations n_0=4(4p0h), n_0 = 5(5p0h) and n_0 =6(5p1h) respectively. It is observed that Weisskopf-Ewing estimates as well as hybrid model predictions are failed to account the compound nucleus peak (maximum). The values predicted by theory are overestimated by an order of magnitude. This is due to the fact that yields of nuclides with closed or nearly closed nucleon shells are not predicted well when standard Fermi gas level densities are used in the evaporation phase of the deexcitation calculation /9,10/. The ^{57}Ni isotopes produced through $^{56}Fe(\alpha,3n)$ reaction, is corresponding to the closure of $f_{7/2}$ shell for protons.

Kataria et al /4/ incorporated a shell dependent level density formula due to Kataria, Ramamurthy and Kapoor /5/ in the ALICE code/2/. This model relates the shell effects in the nuclear level densities to the shell correction term of the nuclear mass surface. The comparison of experimental results was also made using shell dependent level density formula(KRK) and shown in figure V.11. It is observed that shell dependent level density option gives better description of experimental results. This indicates that the reaction yield for ^{57}Ni nucleus is sensitive to nuclear structure, where shell closure occurs at $f_{7/2}$ shell.

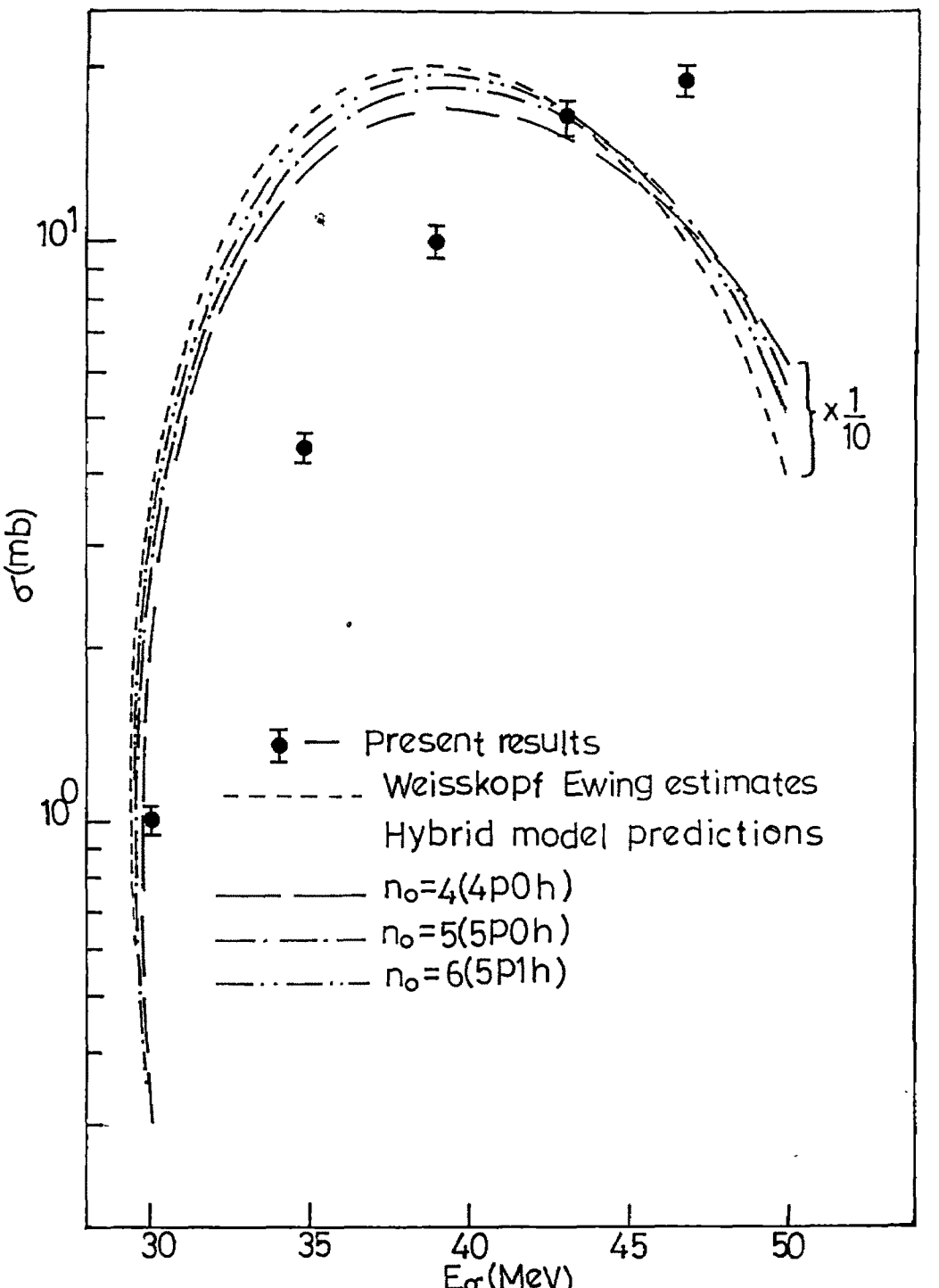

Fig.V.10 COMPARISON OF THEORETICAL AND EXPERIMENTAL EXCITATION FUNCTION OF $^{56}Fe(\alpha,3n)^{57}Ni$ REACTION

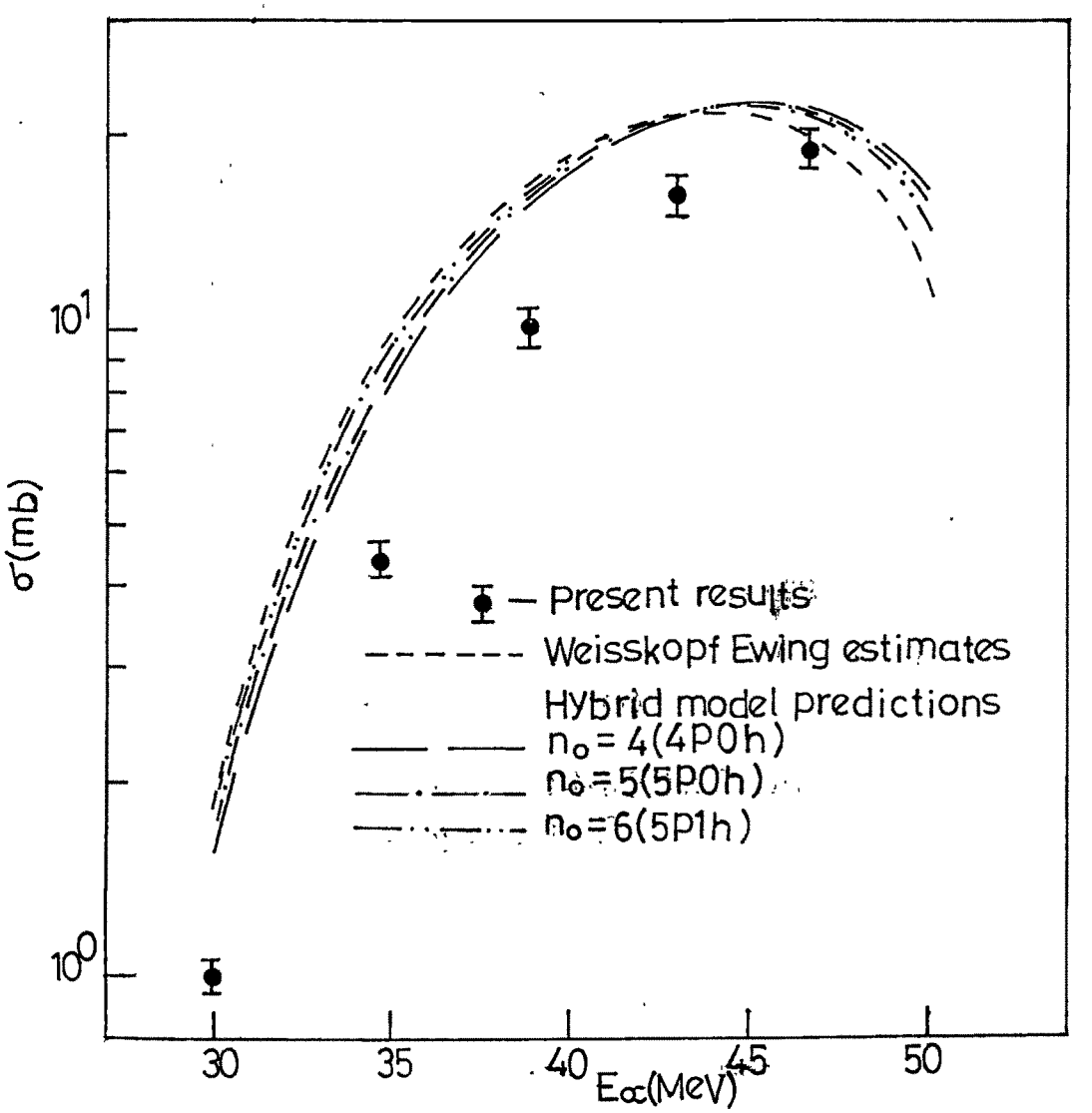

Fig.V.11 COMPARISON OF THEORETICAL AND EXPERIMENTAL EXCITATION FUNCTION OF $^{56}Fe(\alpha,3n)^{57}Ni$ REACTION

(ii) $^{56}Fe(\alpha,4n)^{56}Ni$ reaction :

The product nucleus ^{56}Ni produced through $^{56}Fe(\alpha,4n)$ reaction, has shell closure at $f_{7/2}$ shell for both neutrons and protons. The experimental excitation function together with theoretical predictions considering both the options of level density are shown in figures V.12 and V.13 respectively. It is observed that the shell dependent level density (KRK) option gives better description of results over the standard Fermi gas option. However the cross sections obtained with KRK option are lower by a factor of five.

Owing to the large threshold energy (39.17 MeV) and limited projectile energy (E_α=50 MeV), we have studied only the rising part of the excitation function. In this region preequilibrium model predictions are not very sensitive as the compound nucleus mechanism dominates due to limitations of bombarding energy.

From the study of the above presented, eleven reactions of (α,xn) type induced in light, medium and heavy nuclei, the following general conclusions may be drawn:

1) Essentially the same basic mechanism governs the emission of neutrons from light, medium and heavy nuclei.

2) For bombarding energies within about 10-15 MeV from the reaction threshold, single as well as multiple emission of neutron is governed by the well known compound nucleus evaporation mechanism and is adequately accounted for by simple or multistep Weisskopf-Ewing formalism.

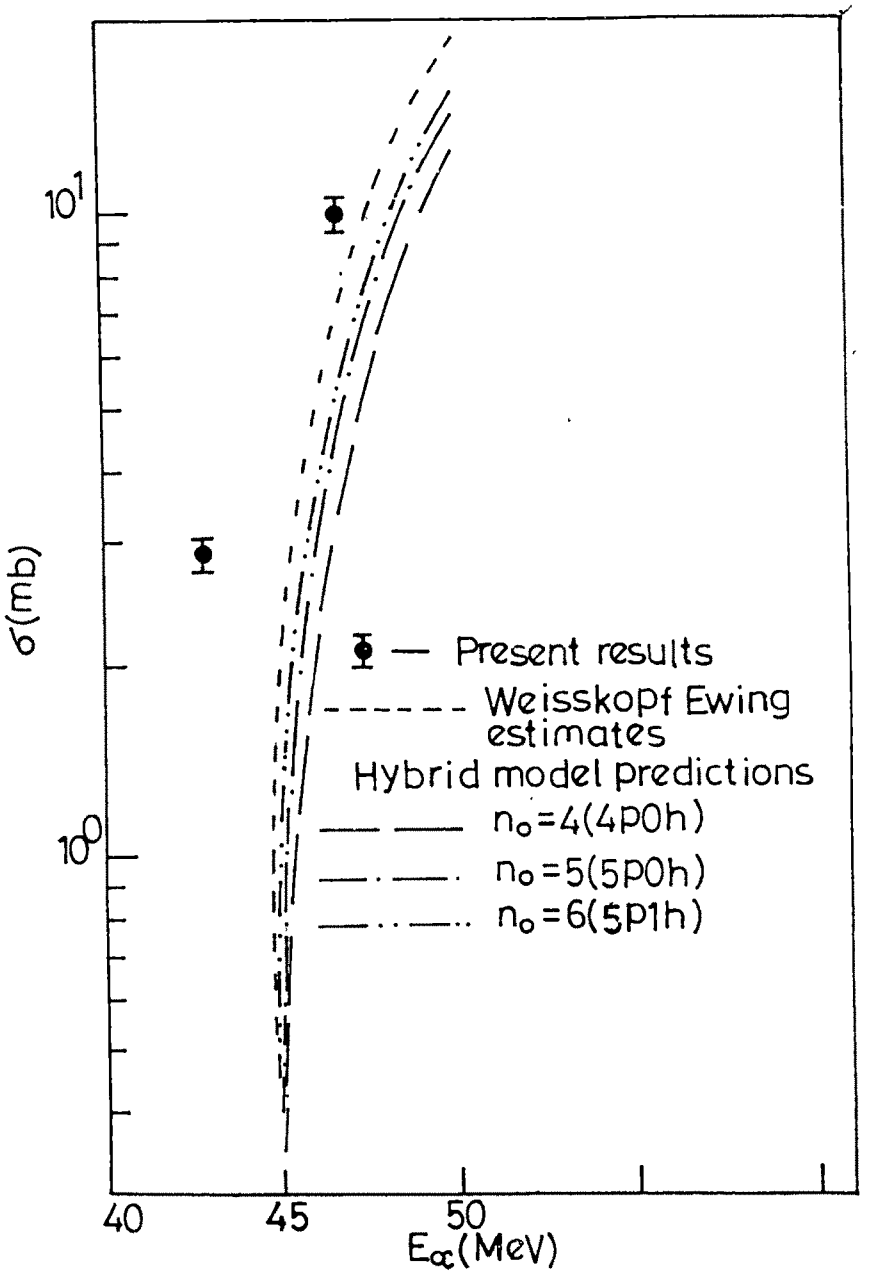

Fig.V.12 COMPARISON OF THEORETICAL AND EXPERIMENTAL EXCITATION FUNCTION OF $^{56}Fe(\alpha,4n)^{56}Ni$ REACTION

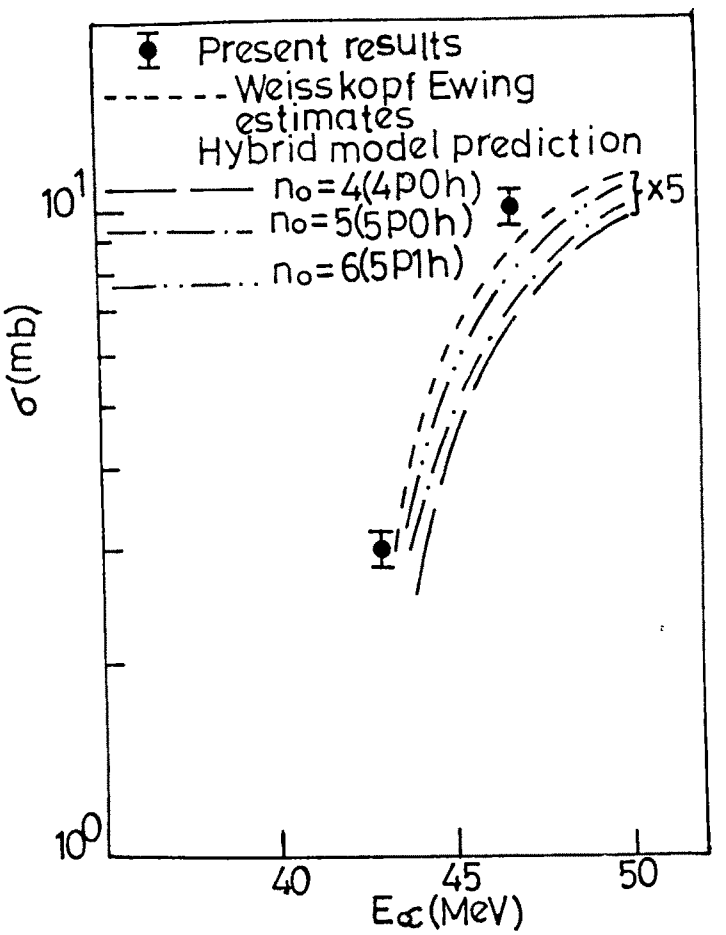

Fig.V.13 COMPARISON OF THEORETICAL AND EXPERIMENTAL EXCITATION FUNCTION OF $^{56}Fe(\alpha,4n)^{56}Ni$ REACTION

3) At increasing energies the unambiguous evidence for increasing non-compound contributions in (α,xn) reactions particularly for decreasing neutron multiplicity.

4) The emission of neutrons from nuclear systems at excitation energies beyond a few tens of MeV is caused by the preequilibrium decay of the system in a time much shorter than the time for evaporation from an equilibrated compound nucleus. This is rather indirectly indicated by the "high energy tails" of the experimental excitation functions which signify a less rapid fall of the cross section than predicted by compound nucleus model.

5) The shape of the excitation functions in the preequilibrium dominated regions of energy is well reproduced by the improved version of Hybrid model. As far as the magnitudes of the cross sections are concerned, there is a reasonable agreement with the predictions of this model using an initial exciton configuration n_0=4(4p0h) i.e. pure particle state.

6) The above initial configuration justifiable implies the assumption that following the first projectile-target interaction only four excitons share the excitation energy, they being naturally the four nucleons of the α-particle. This view is quite consistent with the basic physics of the preequilibrium mechanism that only a few degrees of freedom is initially excited in a nuclear reaction at moderate energy.

7) It has been observed that reaction yields of nuclides with closed or nearly closed shells are predicted well with shell dependent level density option. It means that these nuclides show nuclear structure effects.

V.2 (α,pxn) Type of Reactions

If one neglects the isospin dependence of nuclear forces, which accounts for the Coulomb interactions and assumes the indistinguishablility of the proton and neutron from a nuclear point of view, then this class of reactions could be merged with the previous class. However, from view point of nucleon emission it is useful to discuss the (α, pxn) reactions as a separate group, because of the profound importance of the Coulomb field on the emissions of protons and also because of the basic structural aspect that there is a invariably a neutron excess over protons in the concerned nuclei.

V.2.1 Target Element Gold:

(i) $^{197}Au(\alpha,2pn)^{198}Au$ reaction :

Figure V.14 shows the excitation function for Au(α,2pn) and Au(α,3n) reactions. At the outset it can be seen that the shape of the experimental excitation function is very different from the general shape of the excitation function for the (α,xn) type of reactions. Further more, the magnitude of cross sections are also generally down by one or two orders of magnitude. This as indicated above, is due to the appearance of protons in the outgoing channel, with a multiplicity of two in the present case.

It would be interesting to compare the excitation function for this reaction with that of the earlier presented $^{197}Au(\alpha,3n)^{198}Tl$ reaction. Both the reactions differ in the replacement of two neutrons by two protons in the outgoing group of three nucleons in each reaction. The difference in shapes as well as in magnitudes,

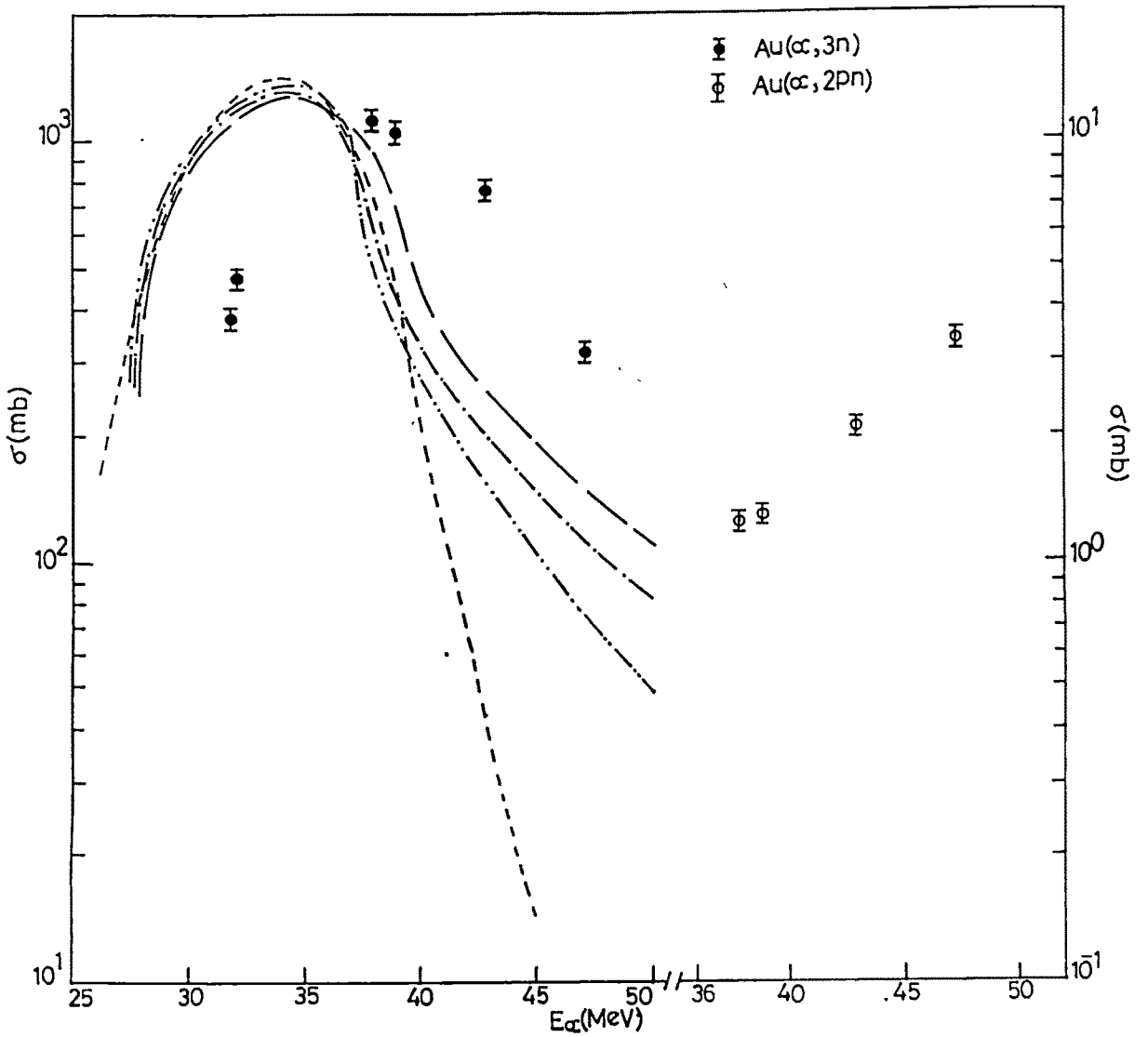

Fig.V.14 COMPARISON OF EXCITATION FUNCTIONS FOR Au(α,3n) AND Au(α,2pn) REACTIONS

consequent on this change is very striking. In physical terms, these differences are not only attributable to the influence of the Coulomb field, but also to specifically nuclear differences between the proton and neutron, such as the isospin.

The observed experimental cross sections between 30 to 50 MeV can not be accounted by theoretical predictions. This can be understood as being due to the strong inhibition of low energy protons, owing to the large Coulomb barrier offered by the compound nucleus to the evaporation of charged particles from it.

V.2.2 Target Element Antimony :

(i) $^{121}Sb(\alpha,p3n)^{121}Te$ reaction :

Figure V.15 shows the experimental excitation function for this reaction, together with the theoretical ones based on Weisskopf-Ewing estimates and Hybrid model predictions for n_0=4, 5 and 6 respectively.

Owing to large threshold energy for $^{121}Sb(\alpha,p3n)^{121}Te$ reaction (i.e 31.17 MeV) and as such there are only a few points in the initial rising part of the experimental excitation function. In this region the preequilibrium model predictions are not very sensitive as the compound nucleus mechanism dominates.

It can be seen from figure that compound nucleus peak underestimated by a factor of more than three. This is due to the pair of reactions $^{121}Sb(\alpha,4n)^{121}I$ and $^{121}Sb(\alpha,p3n)^{121}Te$. Both products being neutron deficient isotopes, naturally the isobar with higher Z decays to that of the lower Z by β^+ emission and/or electron capture. Thus, since both these reactions are energetically possible (their threshold differ by a couple of MeV) in activation measurements, the cross sections

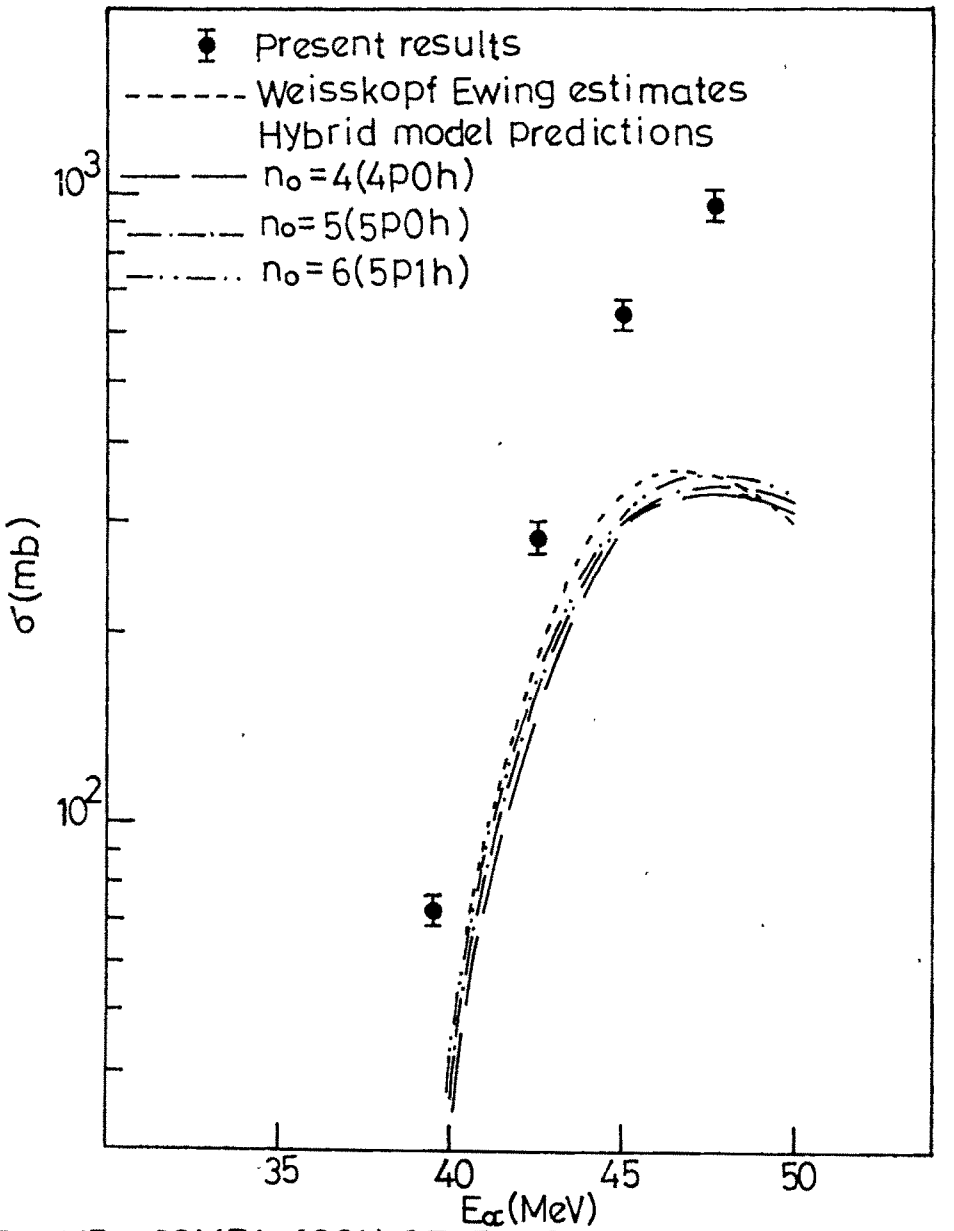

Fig.V.15 COMPARISON OF THEORETICAL AND EXPERIMENTAL EXCITATION FUNCTION OF $^{121}Sb(\alpha,p3n)^{121}Te$ REACTION.

determined for the lower Z isobar always include the contributions from higher Z isobar. This is evident from the nearly identical values of the cross sections for $^{121}Sb(\alpha,4n)$ (figure V.8) and $^{121}Sb(\alpha,p3n)$ reactions. The interfering contribution to the $(\alpha,p3n)$ cross sections from that of $(\alpha,4n)$ reaction is really a major problem specially in view of the fact that the latter cross section is generally ten times larger than the former.

V.2.3 Target Element Iron:

(i) $^{56}Fe(\alpha,pn)^{58}Co$ reaction :

Figures V.16 and V.17 show the present experimental results together with theoretical calculations based on Weisskopf-Ewing estimates as well as Hybrid model predictions considering Fermi gas level density option and shell dependent level density (KRK) option respectively. It can be seen at once that, because the Coulomb barrier is, comparatively small for iron than antimony and gold , the "compound nucleus bump" is just evident in the experimental excitation function. Also the compound nucleus contributions are significant upto a high energy of about 28 MeV.

The residual nucleus ^{58}Co, produced through $^{56}Fe(\alpha,pn)$ reaction, has 27 protons which is nearer to the closure of the $f_{7/2}$ shell. It has long been known that yields of nuclides with closed shell or nearly closed nucleon shells are not predicted well when standard Fermi gas level densities are used in the "evaporation" phase of the deexcitation calculation/9,10/.

It can be seen from figures V.16 and V.17 that experimental excitation function accounted well with preequilibrium Hybrid model predictions using initial

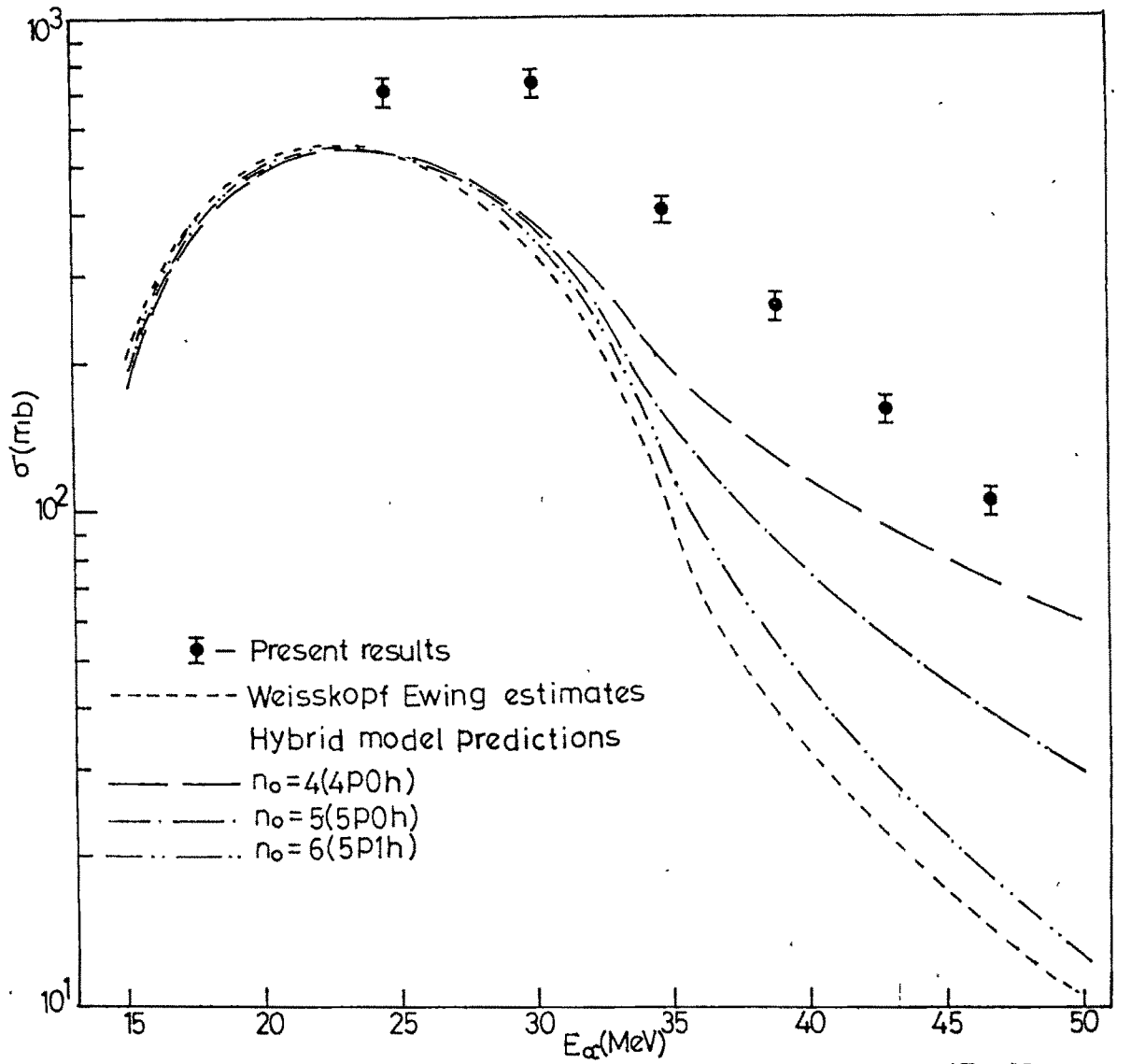

Fig.V.16 COMPARISON OF THEORETICAL AND EXPERIMENTAL EXCITATION FUNCTION OF $^{56}Fe(\alpha,pn)^{58}Co$ REACTION

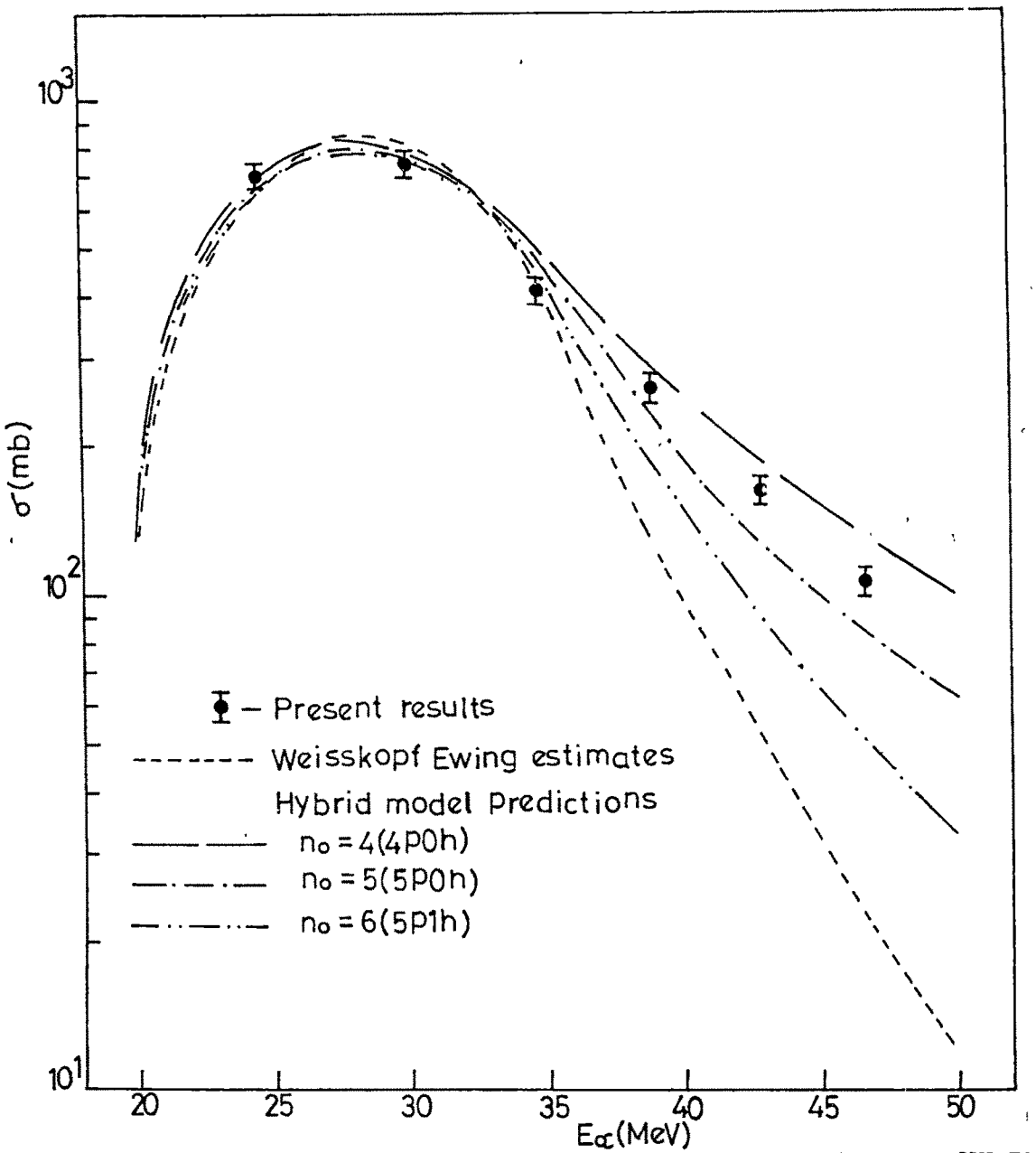

Fig.V.17 COMPARISON OF THEORETICAL AND EXPERIMENTAL EXCITATION FUNCTION OF $^{56}Fe(\alpha,pn)^{58}Co$ REACTION.

exciton number n_0=4(4p0h) and considering shell dependent level density option. The theoretical predictions using initial exciton number n_0=4(4p0h) and considering Fermi gas level density, are lower by a factor of about two and also there is a shift in compound nucleus peak position between theory and experiment. This observation indicates that nuclear shell structure has a profound effect on the level densities of excited nuclei.

(ii) $^{56}Fe(\alpha,p2n)^{57}Co$ reaction :

It is pertinent to compare the excitation function of this reaction with that of $^{56}Fe(\alpha,3n)^{57}Ni$ reaction studied in the present work to asses the influence of Coulomb and isospin effects in the emission of nucleons from light nuclei. These two reactions namely, Fe(α,3n) and Fe(α,p2n) differ only in the replacement of a neutron/proton in the emitted group of nucleons while the excitation function of the former was shown in figures V.10 and V.11, the later is presented in figures V.18 and V.19 together with predictions of Weisskopf Ewing estimates and preequilibrium Hybrid model considering Fermi gas level density and shell dependent level density (KRK) options respectively. Both products being neutron deficient isotopes, naturally the isobar with higher Z decays to that of the lower Z by β^+ emission and/or electron capture. Thus, since both these reactions are energetically possible, the cross section determined for the lower Z isobar always includes the contribution from the higher Z isobar. In the present investigation the excitation function for this reaction is exclusively and carefully calculated using complex cross section formula eqn.13, of Chapter III.3.6.

Figures V.18 and V.19 show the theoretical and experimental excitation functions for this reaction. The difference in shape which is conspicuous in the lower energy part of the excitation function, can be attributed to the negative

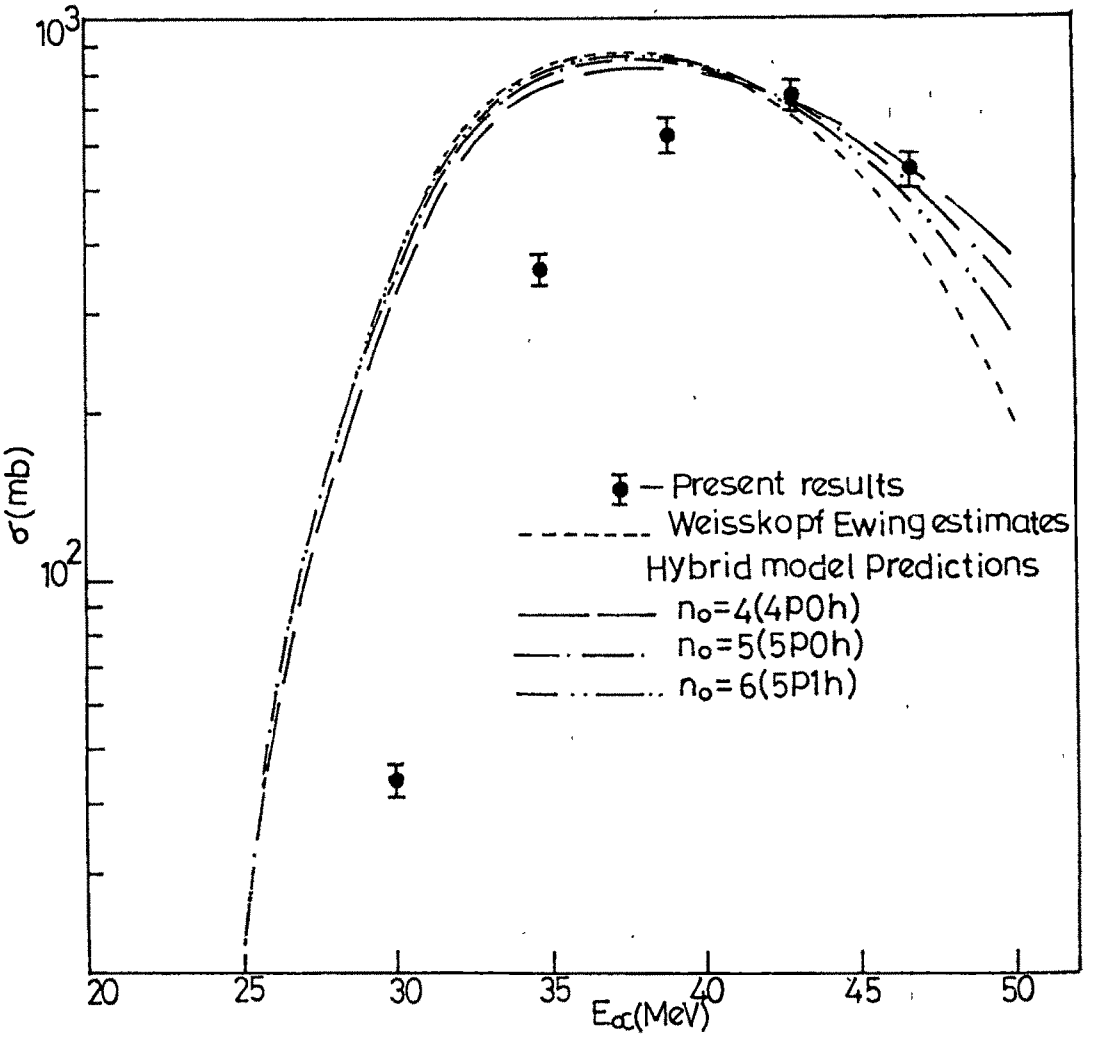

Fig.V.18 COMPARISON OF THEORETICAL AND EXPERIMENTAL EXCITATION FUNCTION OF $^{56}Fe(\alpha,p2n)^{57}Co$ REACTION.

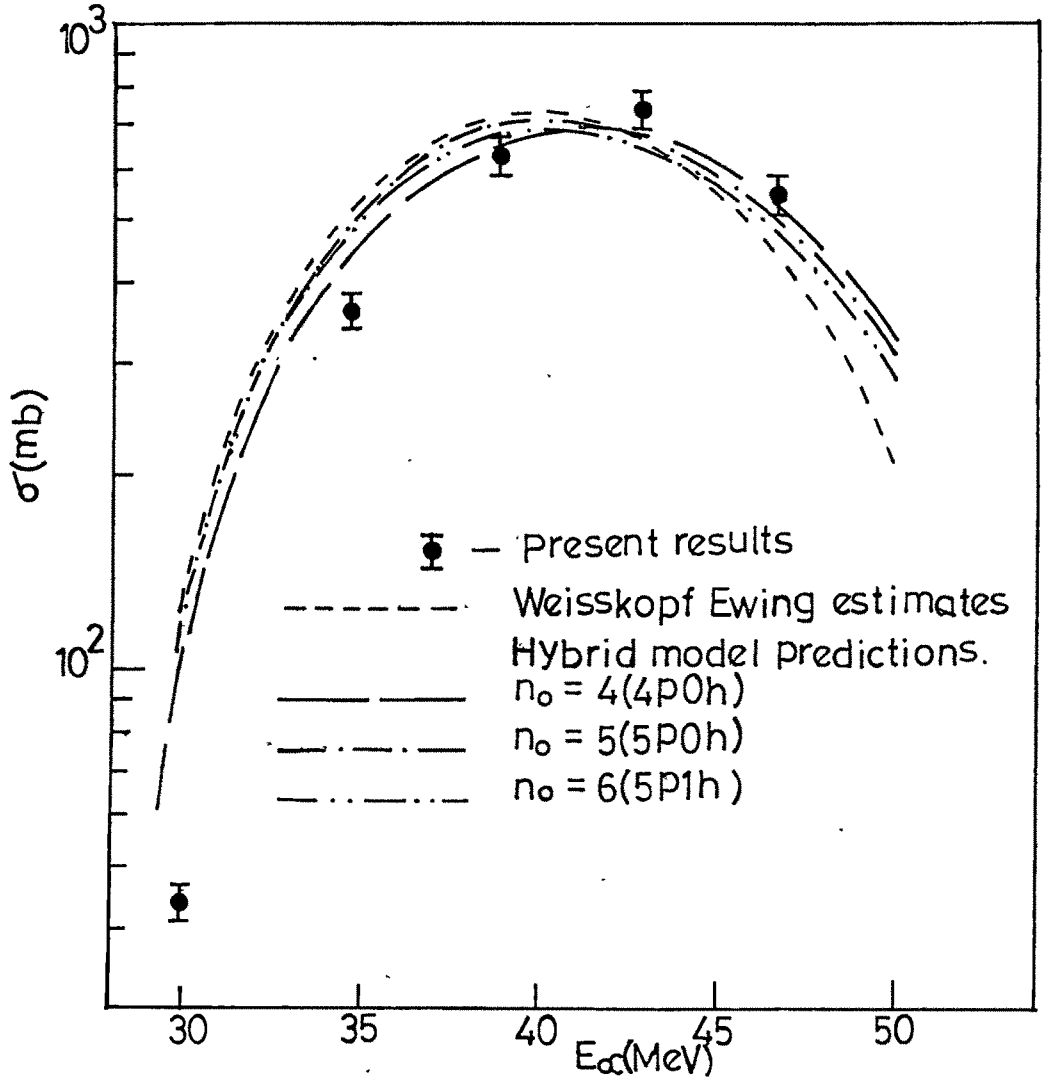

Fig.V.19 COMPARISON OF THEORETICAL AND EXPERIMENTAL EXCITATION FUNCTION OF $^{56}Fe(\alpha,p2n)^{57}Co$ REACTION.

influence of Coulomb barrier on the emission of charged particles. The energy of α-particle is not sufficient to give shape of excitation function beyond compound nucleus peak. Hence, it is not possible to conclude about nuclear differences such as for instance, the isospin.

The shape of the excitation function is fairly well reproduced by the theoretical calculations considering shell dependent level density (KRK) option, since ^{57}Co nucleus has 27 protons which is nearer to closure of the $f_{7/2}$ shell.

(iii) ^{56}Fe(α,p3n)^{56}Co reaction :

Again, it is necessary to compare this reaction with that of ^{56}Fe(α,4n)^{56}Ni reaction studied in the present work. Both products being neutron deficient isotopes, naturally the isobar with higher Z decays to that of the lower Z by β^+ emission and/or electron capture. Thus, since both these reactions are energetically possible, the cross section determined for the lower Z isobar always includes the contribution from the higher Z isobar. In the present investigation the excitation function for this reaction is exclusively and carefully calculated using complex cross section formula eqn.13, of Chapter III.3.6, which is shown in figures V.20 and V.21.

As the threshold energies for ^{56}Fe(α,p3n)^{56}Co reaction is large (36.04 MeV) and as such there are only a few energy points cross section in the initial rising part of the experimental excitation function shown in figures V.20 and V.21 along with theoretical predictions considering Fermi gas level density option and shell dependent level density (KRK) option respectively. In these regions the preequilibrium model predictions are not very sensitive as the compound nucleus mechanism dominates due to the limitations of bombarding energy.It can be seen

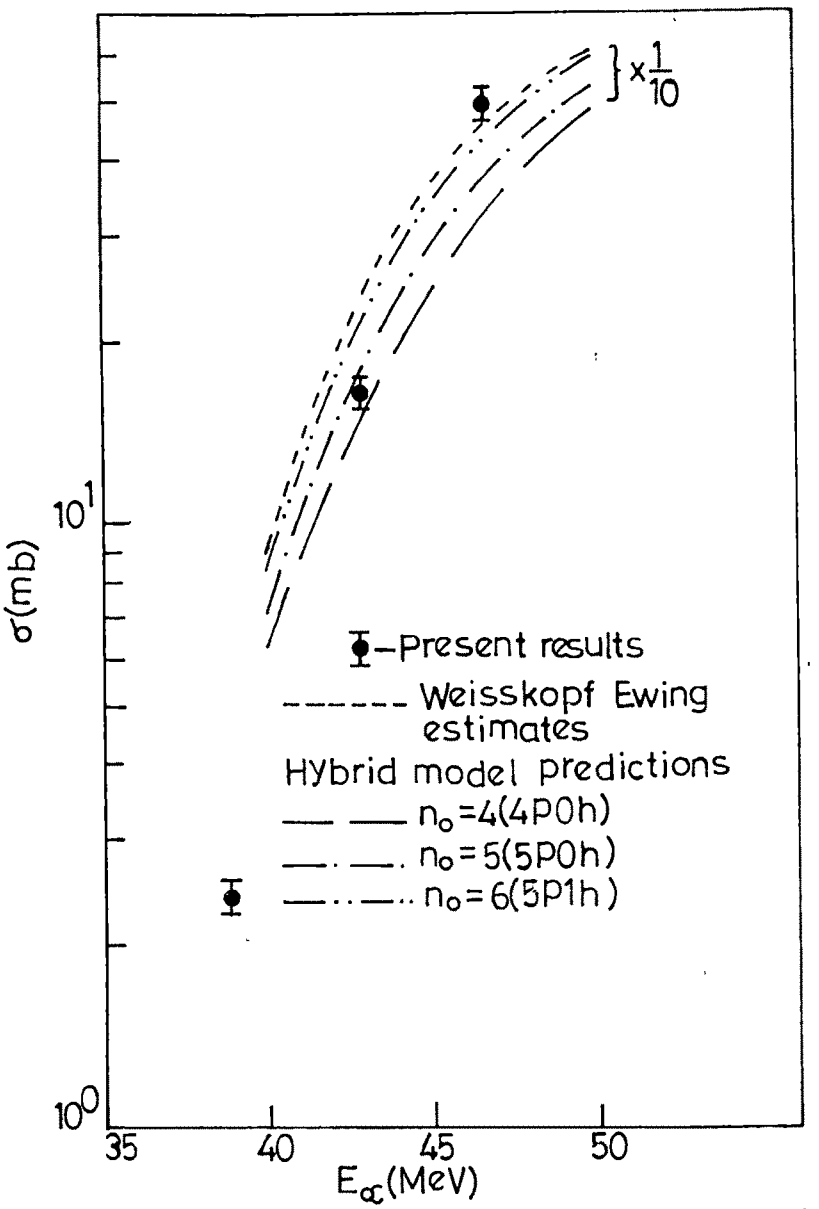

Fig.V.20 COMPARISON OF THEORETICAL AND EXPERIMENTAL EXCITATION FUNCTION OF $^{56}Fe(\alpha, p3n)^{56}Co$ REACTION

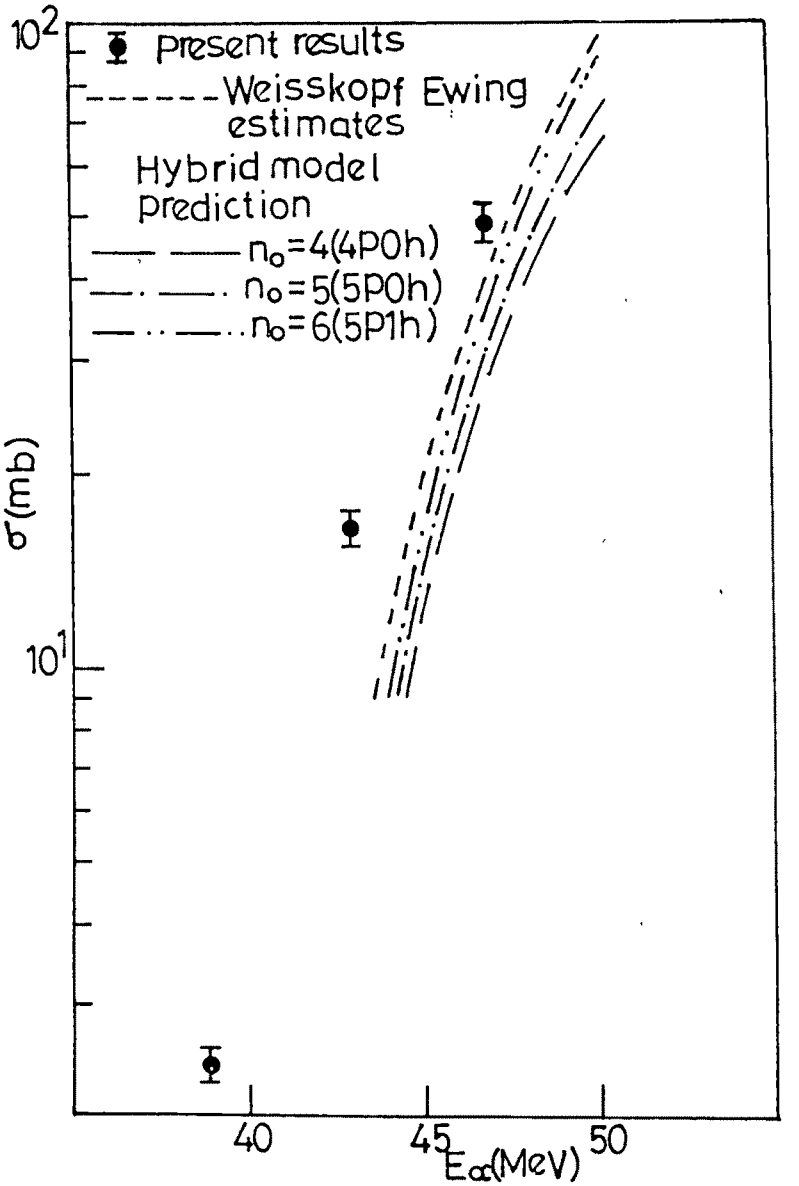

Fig.V.21 COMPARISON OF THEORETICAL AND EXPERIMENTAL EXCITATION FUNCTION OF $^{56}Fe(\alpha, p3n)^{56}Co$ REACTION

that theoretical prediction considering Fermi gas level density option, are overestimated by an order of magnitude as shown in figure V.20.

Summarizing the (α,pxn) type of reactions studied in the present work, it may be inferred that:

1) The cross sections for (α,pxn) type of reactions are, in general, one order of magnitude smaller than those of (α,xn) type of reactions and shapes of excitation functions are significantly different for the two types of reactions.

However, in the case of ^{56}Fe(α,pxn); x=2,3 reactions, the cross sections are significantly higher than that of ^{56}Fe(α,xn);x=3,4 reactions respectively. This indicates that reaction yields are sensitive to nuclear structure. The isotopes ^{56,57}Ni produced through (α,xn) reactions are corresponding to the closure of the $f_{7/2}$ shell for protons in ^{57}Ni and for both protons and neutrons in ^{56}Ni, where as isotopes ^{56,57}Co produced through (α,pxn) reactions are nearly to shell closure of $f_{7/2}$ shell.

2) Due to the limitation of the projectile energy(E_α) and the large effective thresholds energies of these reactions (except for ^{56}Fe(α,pn) reaction), only the predominantly compound nucleus part of the excitation function could be investigated in the present work.

3) The preequilibrium model, when applied to (α,xnyp) type of reactions, drastically failed to account for the magnitude and shape of the observed excitation function by considering Fermi gas level density. However, as observed earlier they do much better when applied to (α,xn) type of reactions, where an equivalent number of neutrons instead of protons and neutrons are emitted.

4) The magnitude as well as shapes of observed excitation function for Fe(α,xnyp) reactions are fairly well reproduced by considering the shell dependent level density instead of Fermi gas level density. This observation indicates that nuclear shell structure has a profound effects on the level density of excited nuclei.

5) The difference in shape which is conspicuous in the lower energy part of the excitation function, can be attribute to the negative influence of Coulomb barrier on the emission of charged particles.

V.3 (α,αxn) Type of Reactions:

The study of α-particle induced reactions in which the α-particle again appears in the out going channel is quite interesting. The obvious implication is the possibility of a direct inelastic scattering as a first step in the reaction mechanism. Further more, as described in Chapter II there are quite contradictory notions about the "pre-formation" or "instant-formation" of the α-particle emitted in these reactions, if it is not a direct inelastic scattering /20/. Although the answers to these questions can be provided only by particle-γ and particle-particle coincident studies, some relevant information can also be obtained from excitation function studies of these reactions.

V.3.1 Target Element Gold :

(i) $^{197}Au(\alpha,\alpha n)^{196}Au$ reaction :

The experimental excitation function for this reaction studied in the present work is shown in figure V.22 together with the theoretical predictions on the basis of

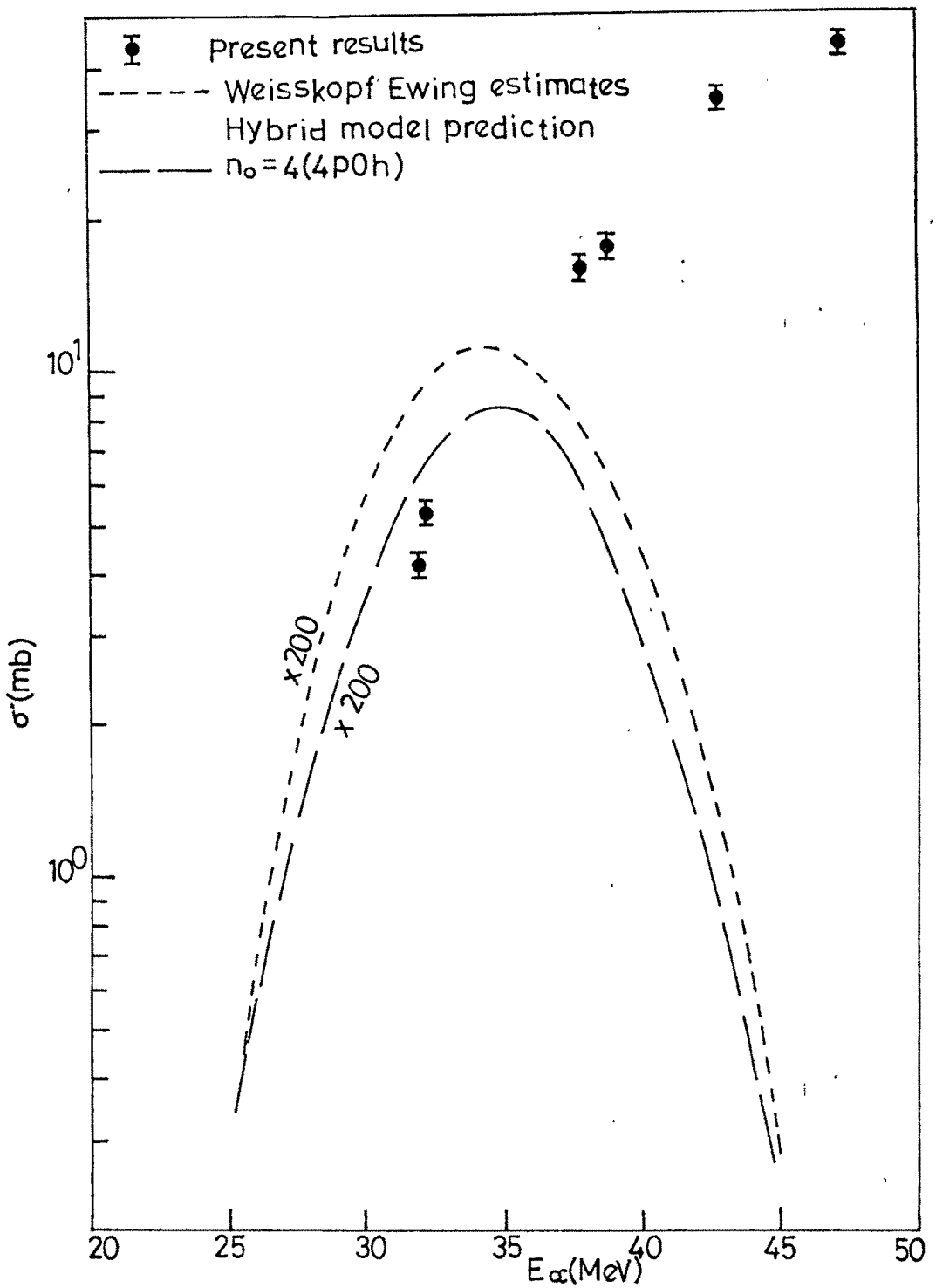

Fig.V.22 COMPARISON OF THEORETICAL AND EXPERIMENTAL EXCITATION FUNCTION OF $^{197}Au(\alpha,\alpha n)^{196}Au$ REACTION.

Weisskopf-Ewing estimates and Hybrid model. It was observed that Weisskopf Ewing estimates are down by two order of magnitudes, showing the insignificance of compound nucleus effects in this reaction.

It can be seen that there is a radical difference in the shape of theoretical and experimental excitation functions. It is also observed that even the preequilibrium hybrid model predictions are down by about two orders of magnitudes.

The only plausible explanation that is left out is the direct interaction effects. The bare structureless shape of the excitation function is itself a pointer to the direct reaction involvement, namely, the inelastic scattering of the incident alpha particle, followed by a neutron evaporation to bring about the observed ($\alpha,\alpha n$) reaction. Similar observations were made by Lanzafame and Blann /19/ while studying this $^{197}Au(\alpha,\alpha n)^{196}Au$ reaction. In their work ,they studied the recoil ranges of the residual nuclei ^{196}Au and found that there is a very little momentum transfer to recoiling nucleus. On this basis they proposed the operation of considerable non-compound mechanism, such as direct interaction and/or preequilibrium decay.

Since, in the present case of $^{197}Au(\alpha,\alpha n)^{196}Au$ reaction, the preequilibrium model has completely failed the inescapable inference seems to be that in this reaction either the alpha particle or the neutron or both may have been emitted in a direct reaction process. This is of course not surprising because, Hybrid model is not designed to deal with alpha particle emission in preequilibrium phase.

V.4 Fraction of Preequilibrium Particle Emission :

The comparison of theory and experiment shows that the preequilibrium process is present in the α-induced reactions and gives a significant contribution.

The preequilibrium fraction (f_{PE}) is a measure of the relative weight of the preequilibrium and equilibrium contribution needed for the production of experimental data . However, the fractions of preequilibrium particle emission for protons and neutrons obtained from the analysis of data are not directly comparable because of the presence of the Coulomb barrier for charged particle emission. The Coulomb barrier tends to cut off the low energy portion of proton spectra and thus reducing the number of equilibrium protons. There is relatively little effect on the number of preequilibrium protons since these tend to be emitted with fairly high energies. The net effect is that as the mass of the compound nucleus increases, the height of the Coulomb barrier increases which decreases the emission of equilibrium proton, and the ratio of preequilibrium to equilibrium proton emission is increased /21/. It is therefore defined as the integral preequilibrium neutron cross section plus preequilibrium proton cross section divided by the total cross section (i.e. equilibrium plus preequilibrium cross sections).

The calculated f_{PE} for ^{56}Fe, ^{113}In, ^{115}In, ^{121}Sb, ^{123}Sb and ^{197}Au are shown in figure V.23, as a function of bombarding energy E_α. It was found that the f_{PE} increases very fast as the energy of the alpha particle increases. Furthermore, it is found that threshold for preequilibrium is higher for the lower mass number and f_{PE} is higher for the system of higher mass number at a given alpha particle energy.

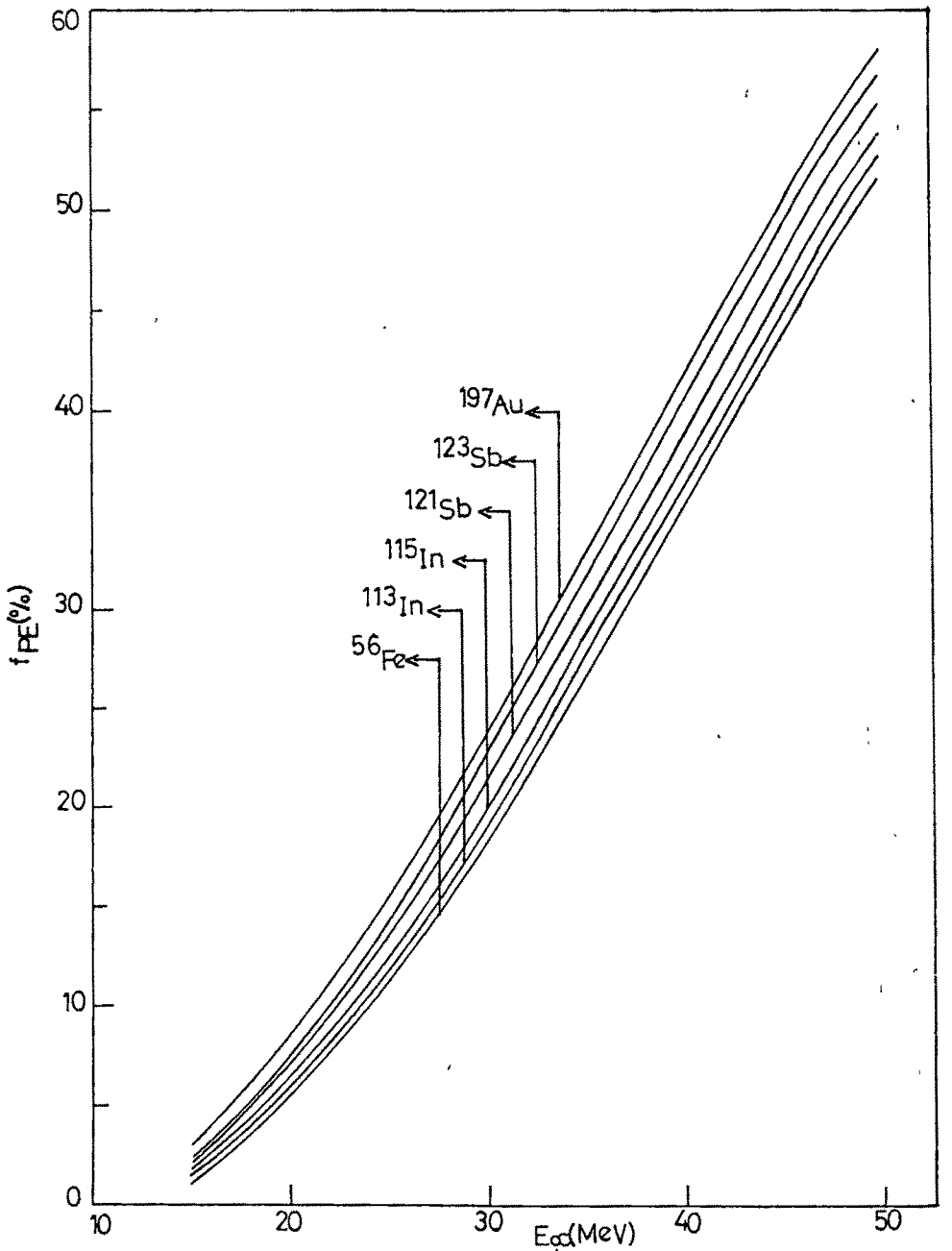

Fig.V.23 f_{PE}(%) for ^{197}Au , ^{121,123}Sb , ^{113,115}In and ^{56}Fe

References:

/1/ M. Blann, Phys. Rev. Lett. **27**, 337 (1971).

/2/ M.Blann,Code ALICE/85/300, Lawrence Livermore National Laboratory Report UCID- 20169 (1984), unpublished.

/3/ M. Blann and H. K. Vonach, Phys.Rev. **C28**, 1475 (1983).

/4/ S.K.Kataria, V.S.Ramamurthy, M.Blann and T.T.Komoto, Nucl.Inst. & Meth. **A288**, 585(1990).

/5/ S.K. Kataria, V.S.Ramamurthy and S. S. Kapoor, Phys. Rev. **C18**, 549 (1978).

/6/ W. D. Myers and W. J. Swiatecki, Nucl. Phys. **81**, 1 (1966).

/7/ F. D. Becchetti and F. D. Greenless, Phys. Rev. **182**, 1190 (1969).

/8/ V.F.Weisskopf and D.H.Ewing, Phys.Rev. **57**,472 (1940).

/9/ N.Rosenzweig, Phys. Rev. **105**,950(1957).

/10/ M. Blann, Nucl. Phys. **80**, 233 (1960).

/11/ M. Blann, Nucl. Phys. **A213**, 570 (1973).

/12/ M. Blann, Ann. Rev. Nucl. Sci. **25**, 123 (1975).

/13/ M. Blann and T.T. Komoto, Phys. Rev. **C29**, 1678 (1984).

/14/ R.Michel and G.Brinkmann, Nucl. Phys. **A333**, 167(1980).

/15/ N.L.Singh, S.Mukherjee, A.V.Mohan Rao, L.Chaturvedi and P.P.Singh, J.Phys. **G21**, 399(1995)

/16/ A. Djalaesis, P. John, H. J. Probst and C. Mayer-Baericke, Nucl. Phys. **A250**, 149 (1975).

/17/ E.Gadidi, E. Gadioli-Erba, L. Sajo-Bohus and G. Tagliaferri, Riv. Nuovo Cimento. **6**,1(1976).

/18/ M.Blann and G.Merkel, Phys. Rev. **B137**,367(1965).

/19/ F.M. Lanzafame and M. Blann, Nucl. Phys. **A142**, 545 (1970).

/20/ E.Gadioli and P.E.Hodgson, Preequilibrium Nuclear Reaction, Oxford, Clarendon, 1992.

/21/ C.K.Cline and M.Blann, Nucl. Phys. **A172**, 225(1971).